What can electron paramagnetic resonance tell us about the Si/SiO₂ system?

P. M. Lenahan[a)]
The Pennsylvania State University, University Park, Pennsylvania 16802

J. F. Conley, Jr.
Dynamics Research Corporation, Beaverton, Oregon 97006

Electron paramagnetic resonance (EPR) measurements of Si/SiO₂ systems began over 30 years ago. Most EPR studies of Si/SiO₂ systems have dealt with two families of defects: P_b centers and E' centers. Several variants from each group have been observed in a wide range of Si/SiO₂ samples. Some of the most basic aspects of this extensive, body of work remain controversial. EPR is an extraordinary powerful analytical tool quite widely utilized in chemistry, biomedical research, and solid state physics. Although uniquely well suited for metal–oxide–silicon (MOS) device studies, its capabilities are not widely understood in the MOS research and development community. The impact of EPR has been limited in the MOS community by a failure of EPR spectroscopists to effectively communicate with other engineers and scientists in the MOS community. In this article we hope to, first of all, ameliorate the communications problem by providing a brief but quantitative introduction to those aspects of EPR which are most relevant to MOS systems. We review, critically, those aspects of the MOS/EPR literature which are most relevant to MOS technology and show how this information can be used to develop physically based reliability models. Finally, we briefly review EPR work dealing with impurity defects in oxide thin films. © *1998 American Vacuum Society.* [S0734-211X(98)08004-4]

I. INTRODUCTION

Electron paramagnetic resonance (EPR)[1] investigations of metal–oxide–silicon (MOS) systems were begun in earnest by Nishi and co-workers[2,3] who identified a paramagnetic defect called the P_b center as a ''trivalent silicon at or very near'' the Si/SiO₂ interface. Nishi *et al.* argued rather persuasively that P_b centers are quite important Si/SiO₂ interface state centers in as processed Si/SiO₂ systems. Later studies refined and reinforced this conclusion.[4–12] P_b centers are silicon ''dangling bond'' centers dominating interface traps at the the Si/SiO₂ boundary. Studies by at least four independent groups indicate a dominating role for P_b centers in several technologically relevant device instabilities.[6–12]

Quite a few MOS oxide centers have also been identified with EPR. The most important centers are E' defects,[8,9,11–14] usually holes trapped at oxygen vacancies. At least five independent groups[8–15] have identified E' defects as dominating deep hole traps in a wide range of oxides. Quite recently, physically based models with considerable predictive power have been developed linking E' defects and molecular hydrogen to P_b dominated Si/SiO₂ interface instabilities.[15,16] In addition to the E' defects, about a dozen nitrogen, phosphorous, and boron related defects have also been identified in MOS oxide systems.[17]

Recently, Stathis and co-workers have strenuously objected to the conclusions drawn in the earlier P_b work.[18,19] On the technologically important (100) Si/SiO₂ interface, the P_{bo} center variant dominates. Stathis and Dori[18] argue that ''the defect responsible for the P_{bo} resonance either is fun-

damentally different from a dangling bond or lies deeper inside the silicon away from the interface.'' Recently Cartier and Stathis[19] wrote that ''prior to these studies, it was widely accepted that the silicon dangling bond defect, which gives rise to the well known P_b signal in electron spin resonance (ESR) is the microscopic defect causing the fast interface state. As will be outlined in this contribution, we cannot support this view.'' They go on to argue that ''silicon dangling bonds, as detected by ESR measurements, account for only a small fraction of the electrically detected interface states.''

Why should we think that the P_{bo} center is a silicon dangling bond? Why should we think that P_b centers play important dominating roles in Si/SiO₂ instabilities? Should we think otherwise?

In order to answer these and other questions, one might simply ask a specialist in the area. However, with a rudimentary understanding of EPR spectroscopy, one may draw conclusions for oneself. In this article we present a brief but quantitative introduction to those aspects of EPR most relevant to MOS studies and a critical review of MOS EPR studies. We show how information gleaned from EPR studies may be utilized to develop physically based predictive models of oxide reliability problems.

II. EPR AND MOS TECHNOLOGY

Advances in MOS technology have resulted in extremely complex integrated circuits with remarkably small device dimensions. With ever greater complexity and with device dimensions approaching the ''atomic'' scale, an approach called building in reliability (BIR) has grown in technologi-

a)Electronic mail: pmlesm@engr.psu.edu

cal importance. BIR involves identifying those device processing parameters that are involved in device failure phenomena and adjusting these parameters in ways that ameliorate or eliminate the failures. This approach holds great promise but for full realization, it requires physically based models of the effects of processing parameters on reliability limiting mechanisms.

With regard to MOS systems, the reliability limiting mechanisms largely involve point defects and point defect interactions: hole trapping, Si/SiO₂ interface trap generation, defect/hydrogen interactions, nitrogen, boron, and phosphorous impurity center responses. These point defects and point defect interactions are generally amenable to studies involving EPR.

Widely utilized by chemists, EPR is an analytical tool which can provide fairly detailed chemical and structural information about trapping centers.[1] It can also provide moderately precise measurements of the densities of these centers, provided that they are paramagnetic. For the relatively simple electrically active defect centers of relevance to MOS device technology, the requirement of paramagnetism is a great advantage. Most trapping centers will capture a single electron or a single hole. Thus, with the capture of either an electron or a hole, an initially diamagnetic center will be rendered paramagnetic and EPR ''active.'' An initially paramagnetic center can be rendered diamagnetic and EPR ''inactive'' with the capture of either an electron or a hole. In this way, EPR can identify the response of a defect to charge carriers, measure its density, and identify its chemical and structural nature.

With a fundamental understanding of the physical and chemical nature of the defects which limit device performance, one may apply the techniques of the statistical mechanics of solids to predict and to manipulate their numbers. EPR is thus directly applicable to the development of physically based BIR models and, arguably, quite technologically useful.

III. EXPERIMENTAL TECHNIQUES

In EPR measurements, the sample under study is exposed to a large slowly varying magnetic field and a microwave frequency magnetic field oriented perpendicularly to the applied field.[1] Usually the measurements are made at an X band: a microwave frequency $\nu \cong 9.5$ GHz.

An unpaired electron has two possible orientations in the large applied field and thus two possible orientation dependent energies. (From classical electricity and magnetism, the energy of a magnetic moment $\boldsymbol{\mu}$ in a magnetic field $\mathbf{H}$ is $-\boldsymbol{\mu} \cdot \mathbf{H}$.) Magnetic resonance occurs when the energy difference between the two electron orientations is equal to Planck's constant, h, times the microwave frequency. For the very simple case of an isolated electron, the resonance requirement may be expressed as

$$h\nu = g_0 \beta_e H, \tag{1}$$

where $g_0 = 2.002319$ and β is the Bohr magneton, $eh/4\pi m_e$, where e is electronic charge and m_e is the electron mass. The Bohr magneton is 9.274015×10^{-28} J/G.

Expression (1) describes the resonance condition for an electron which does not otherwise interact with its surroundings. The structural information provided by EPR is due to deviations from this simple expression. For the relatively simple trapping centers studied in MOS systems, these deviations are due to spin-orbit coupling and electron–nuclear hyperfine interactions.

A. Spin-orbit coupling

The deviations from expression (1) due to spin orbit coupling come about because a charged particle, the electron, traveling in an electric field due to the nuclear charge, experiences a magnetic field $\mathbf{B} = \mathbf{E} \times \mathbf{v}/c^2$, where $\mathbf{E}$ is the electric field, $\mathbf{v}$ is the velocity, and c is the speed of light.[1] The spin-orbit interaction may be understood *qualitatively* (and *only* qualitatively) in terms of the Bohr picture: an electron moves about the nucleus in a circular orbit. It would appear to an observer on the electron that the positively charged nucleus is in a circular orbit about the electron. (It appears to an unsophisticated observer on earth that the sun is in a circular orbit about the earth.) The nucleus thus generates a local magnetic field which would scale with the electron's orbital angular momentum, $\mathbf{r} \times \mathbf{p}$, and with the nuclear charge. One would thus correctly surmise that spin-orbit coupling interactions increase with increasing atomic number and orbital angular momentum quantum number.

In solids, the spin-orbit interaction is ''quenched'' but a second order effect appears from excited states. This effect scales with the applied magnetic field and depends on the orientation of the paramagnetic defect in the applied magnetic field. The spin-orbit coupling may thus be included in the EPR resonance condition by replacing the constant g_0 of expression (1) with a second rank tensor g_{ij}. The symmetry of this tensor reflects the symmetry of the paramagnetic center. Under some circumstances, the symmetry of the tensor may permit identification of the defect under study.

Perturbation theory allows calculation (with modest accuracy) of the g tensor for the simple defects so far studied in MOS systems.[1] The components of the g tensor are given by

$$g_{ij} = g_0 \delta_{ij} - 2\lambda \sum_k \frac{\langle \alpha | L_i | k \rangle \langle k | L_j | \alpha \rangle}{(E_k - E_\alpha)}. \tag{2}$$

Here, g_0 is the free electron value, λ the atomic spin-orbit coupling constant, L_i and L_j are angular momentum operators appropriate for the x, y, or z directions, and the summation is over all excited states k. State $|\alpha\rangle$ and energy E_α correspond to the paramagnetic ground state of the system.

B. Electron–nuclear hyperfine interactions

The other important source of deviation from expression (1) is the hyperfine interaction of the unpaired electron with nearby nuclei.[1,20] Certain nuclei have magnetic moments; in metal/insulator/silicon systems, the significant magnetic nuclei are ^{29}Si (spin 1/2), ^{1}H (spin 1/2), ^{31}P (spin 1/2), and ^{14}N
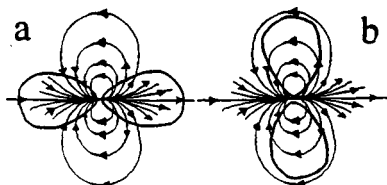
FIG. 1. Schematic illustration of an electron in a p orbital interacting with a magnetic nucleus (a) for the nuclear moment parallel to the symmetry axis and (b) perpendicular to the symmetry axis.

FIG. 2. Schematic of the isotropic interaction of an s orbital electron with a magnetic nucleus.

(spin 1). (Boron, with two stable magnetic nuclei, has been a minor factor in EPR studies of insulating films on silicon.) A spin 1/2 nucleus has two possible orientations in the large applied field; a spin 1 nucleus three possible orientations. Each nuclear moment orientation corresponds to one local nuclear moment field distribution.

We envision the nuclear moment interacting with an unpaired electron residing in a wave function which is a linear combination of atomic orbitals (LCAOs). For the defects of interest in MOS systems, we need only consider s- and p-type wave functions. The LCAO for an unpaired electron can be written as

$$|\alpha\rangle = \sum_n a_n\{c_s|s\rangle + c_p|p\rangle\}, \tag{3}$$

where $|s\rangle$ and $|p\rangle$ represent the appropriate atomic orbitals corresponding to the nth site, a_n^2 represents the localization on the nth site, and c_s^2 and c_p^2 represent, respectively, the amount of s and p character of the wave function on the nth atomic site.

For the most important MOS oxide and interface sites, $a_1^2 \cong 1$; that is, the unpaired electron is reasonably well localized at a single nuclear site. (For all but one of the defects discussed in this article, $0.6 < a_1^2 < 1$.) To first order then, we can interpret EPR spectra in terms of s/p hybridized atomic orbitals localized at a central site.

The electron nuclear interaction of an electron in a p orbital is anisotropic: a classical magnetic dipole interaction is schematically illustrated in Fig. 1. The interaction is strongest when the field is parallel to the symmetry axis. The sign of the interaction changes and the magnitude is decreased by one half when the field is perpendicular to the symmetry axis.

When the electron and nuclear moments are aligned by a strong magnetic field in the z direction, a reasonable assumption for work discussed in this article, only the z component of the dipolar field is important, because the interaction energy involves a dot product. $-\boldsymbol{\mu}\cdot\mathbf{H}$. This z component, $g_n\beta_n(1 - 3\cos^2\theta)r^{-3}$, is averaged over the electronic wave function to produce the dipolar contribution,

$$\text{Dipolar contribution} = -g_n\beta_n\left\langle\frac{1 - 3\cos^2\theta}{r^3}\right\rangle. \tag{4}$$

The electron–nuclear hyperfine interaction of an electron in an s orbital is isotropic. This interaction is illustrated in Fig. 2. Th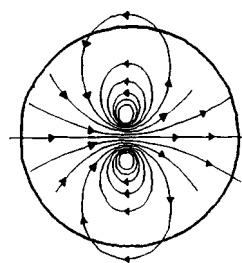e spherical symmetry of the orbital results in zero interaction with this field except for a spherical region about the nucleus with a radius of an imaginary current loop generating the nuclear moment's field. Since the s orbital has a nonzero probability density at the nucleus, a large isotropic interaction results. The s orbital hyperfine interaction can also be computed from an elementary electricity and magnetism calculation:[21] the magnetic field at the center of a current loop of radius a is given by $2\mu/a^3$, where μ is the magnetic moment of the current loop. The probability density of the electron varies little over the volume of the nucleus; take it to be constant, $|\alpha(0)|^2$. Considering then only the fraction of the electron wave function at the nucleus, to be $\frac{4}{3}\pi a^3|\alpha(0)|^2$, the interaction would be

$$A(\text{isotropic}) = \left(\frac{4}{3}\pi a^3|\alpha(0)|^2\right)\left(\frac{2\mu}{a^3}\right). \tag{5}$$

The magnetic moment of the nucleus is the nuclear g factor, g_n, times the nuclear Bohr magneton, β_n. Thus, the isotropic or Fermi contact interaction is given by

$$A_{\text{iso}} = \frac{8\pi}{3}g_n\beta_n|\alpha(0)|^2, \tag{6}$$

where $|\alpha(0)|^2$ represents the unpaired electron probability density at the nucleus.

Both isotropic and anisotropic hyperfine interactions are present for nearly all the paramagnetic centers studied in amorphous thin films on silicon. (The sole exception is atomic hydrogen.) This is so because the unpaired electron wave functions generally involve both p-orbital and s-orbital character. The hyperfine interactions, like the spin-orbit interactions, are expressed in terms of a second rank tensor. To a pretty good approximation, the centers in these films have axially symmetric wave functions and thus an axially symmetric tensor is appropriate.

With the magnetic field parallel to the p orbital symmetry axis, the anisotropic coupling of Eq. (4) yields $(4/5)g_n\beta_n\langle r^{-3}\rangle$; the field perpendicular to the symmetry axis results in an interaction of half the magnitude and opposite sign $-(2/5)g_n\beta_n\langle r^{-3}\rangle$. This result is intuitively satisfying and consistent with the sketches of Fig. 1.

The components of the hyperfine tensor correspond to sums of the isotropic and anisotropic interactions for the applied field parallel and perpendicular to the unpaired electron's orbital symmetry axis:
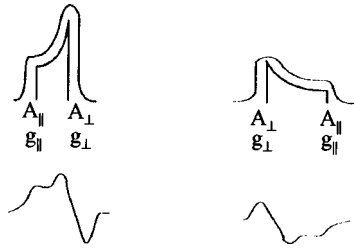
FIG. 3. Schematic sketch of the EPR spectrum of a spin-1/2 nucleus system with axial symmetry. (a) illustrates a random array of identical defects with a solid line and a random array in an amorphous matrix with a dotted line. (b) illustrates the derivative of the amorphous absorption pattern.

$$A_{\parallel} = A_{iso} + 2A_{aniso}; \tag{7}$$

$$A_{\perp} = A_{iso} - A_{aniso}, \tag{8}$$

where

$$A_{aniso} = \tfrac{2}{5} g_N \beta_N \langle r^{-3} \rangle. \tag{9}$$

For a paramagnetic center with a specific orientation (designated by the angle θ between the symmetry axis and the applied field vector) the resonance condition is

$$H = H_0 + M_1 A, \tag{10}$$

where $H_0 = h\nu/g\beta_e$, and M_1 is the nuclear spin quantum number,

$$g = (g_{\parallel}^2 \cos^2 \theta + g_{\perp}^2 \sin^2 \theta) \tag{11}$$

and

$$A = (A_{\parallel}^2 \cos^2 \theta + A_{\perp}^2 \sin^2 \theta). \tag{12}$$

Equations (10)–(12) provide a very straightforward basis for analyzing EPR results for defects with a specific orientation with respect to the applied magnetic field. The "dangling bond" centers at the Si/SiO$_2$ boundary yield spectra readily described by expressions (10)–(12) since the crystallinity of the silicon substrate provides a fixed relationship between the applied field and defect orientation.

The description of EPR spectra of defects within an amorphous film is more complex. All defect orientations are equally likely and, due to the lack of long range order, slight differences in local defect geometry may be anticipated. The presence of defects at all orientations leads to the continuous distribution of both g and A values from $g_{\parallel}$ and $A_{\parallel}$ to $g_{\perp}$ and $A_{\perp}$. The differences in local geometry lead to slight defect-to-defect variations in $g_{\parallel}$, $g_{\perp}$, $A_{\parallel}$, and $A_{\perp}$.

Both of these complications are relatively easy to deal with. The random distribution of defect orientation can be dealt with easily in terms of analytical expressions found in most EPR textbooks. (For axially symmetric centers, far fewer centers will have the symmetry axis parallel to the applied field than perpendicular to it; thus the EPR spectrum intensity will be far stronger at the $A_{\perp}$ and $g_{\perp}$ values than at $A_{\parallel}$ and $g_{\parallel}$.) The slight defect-to-defect variations in g and A values lead to broadening of the line shapes anticipated for unbroadened tensor components. (The process is illustrated in Fig. 3.)
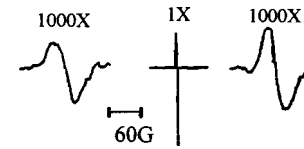

FIG. 4. EPR trace of the E' center showing a very narrow center line trace corresponding to the $\approx$95% abundant spin-zero ^{28}Si nuclei and two broad lines corresponding to the $\approx$5% abundant spin-1/2 ^{29}Si nuclei.

The evaluation of EPR hyperfine tensor components allows for a reliable and moderately precise identification of the unpaired electron's wave function.

For reasonably "clean" MOS oxides, we anticipate significant concentrations of only silicon, oxygen, hydrogen, and under certain circumstances, nitrogen, phosphorous, and boron. The nuclear moments of these atoms are all quite different.[1] Over 99% of oxygen atoms have nuclear spin zero; 95% of silicon atoms also have spin zero but about 5%, those with ^{29}Si nuclei have a nuclear spin of one half. This 95% spin zero/5% spin one half ratio is unique among elements of the periodic table. Thus, a three line pattern with two side peaks, each about 2.5% the integrated intensity of the much more intense center line, can be convincingly linked to an unpaired electron on a silicon atom. Hydrogen nuclei (99.9% of them) have a nuclear spin of one half and thus produce a two line spectrum. Nitrogen nuclei (99.6% of them) have a nuclear spin of one and therefore produce three lines of equal intensity.

A little common sense usually allows one to identify the magnetic nuclei involved in observed hyperfine interactions. Having identified the nuclear species involved, a first order analysis of the unpaired electron wave function is extremely straightforward in terms of the LCAO picture. For defects in a crystalline environment, Eq. (12) can be fit to the EPR spectrum for several values of θ. For defects in an amorphous (or polycrystalline) environment one may fit the appropriately broadened analytical expressions to the EPR spectra to yield $A_{\perp}$ and $A_{\parallel}$. (This process is illustrated in Fig. 3.) Using Eqs. (7) and (8) one then obtains the isotropic and anisotropic coupling constants A_{iso} and A_{aniso}.

Tabulated values[1] of A_{iso} and A_{aniso} calculated for 100% occupation probability can then be utilized to determine the hybridization and localization of the electronic wave functions. For example, the isotropic and anisotropic coupling constants for an electron 100% localized in a silicon s and p orbital are, respectively, $a_o = 1639.3$ G and $b_o = 40.75$ G. In Fig. 4, we illustrate an EPR trace of the E' center, the dominating deep hole trap in high quality thermally grown oxides on silicon. An application of the analysis schematically indicated in Fig. 2 indicates that $A_{iso} = 439$ G and $A_{aniso} = 22$ G. If the electron were 100% localized in a silicon s orbital, we would expect an isotropic coupling constant of $a_o = 1639.3$ G. We measured 439 G; thus the orbital has $439/1639 \cong 27\% s$. If the electron were 100% localized in a silicon p orbital we would expect $A_{aniso} = b_o = 40.75$ G. We measured $\cong 22$ G; thus, the orbital has $22/40.75 \cong 54\% p$. The analysis indicates a localization on the center silicon of

about $(54+27)=81\%$. Although the crude analysis just discussed is not extremely precise it is, to first order, *quite* reliable. One should realize that the isolated atomic values obtained for a_o and b_o are themselves only moderately accurate and that placing a silicon atom in an oxide matrix will inevitably alter the constants somewhat. Nevertheless, a straightforward analysis of hyperfine parameters provides moderately accurate measurement of hybridization and localization.

IV. MEASUREMENT OF DEFECT DENSITIES

A. Accuracy and sensitivity

The EPR is typically measured by placing the sample and a calibrated spin standard in a high Q microwave cavity. EPR is detected via changes in Q: Comparing sample and standard responses, relative defect densities can be determined to a precision of better than $\pm 10\%$; absolute precision is better than a factor of 2. With considerable effort, as few as $\cong 10^{10}$ defects/cm² may be observed using standard EPR. As discussed later in the text, the EPR detection technique called spin dependent recombination is about $\sim 10^7$ times more sensitive than conventional EPR. Unfortunately quantitative spin counting measurements are not yet possible via spin dependent recombination.

V. PARAMAGNETIC CENTERS IN MOS SYSTEMS

A. Si/SiO₂ interface defects: P_b centers

1. Analysis of the structure

The chemical and structural nature of P_b centers has been established by several independent, consistent, and mutually corroborating studies. Three P_b variants have been consistently observed: at (111) Si/SiO₂ interfaces a defect called simply P_b, at (100) Si/SiO₂ interfaces two defects called P_{b0} and P_{b1}. The structure of both the (111) Si/SiO₂ P_b and the (100) Si/SiO₂ P_{b0} are reasonably well understood; only a rudimentary understanding of P_{b1} exists at this time.

P_b centers were first observed by Nishi and co-workers[2,3] in a study initiated more than 30 years ago. Their work focused primarily on the (111) Si/SiO₂ system. They showed that the P_b centers were at or very near to the Si/SiO₂ interface and that they possess an axially symmetric g tensor $g_\parallel \cong 2.000$ and $g_\perp \cong 2.01$ with the symmetry axis corresponding to the (111) direction. On the basis of this information Nishi *et al.* concluded that P_b centers are "trivalent silicon" centers at or very near the Si/SiO₂ boundary.

Later, Poindexter *et al.*[4,5] obtained more precise g tensor parameters. For the (111) Si/SiO₂ P_b, they found $g_\parallel \cong 2.0014$ and $g_\perp \cong 2.0081$ with, as Nishi had observed previously, the symmetry axis corresponding to the Si(111) direction. For the (100) Si/SiO₂ system, they found two P_b variants; P_{b0} and P_{b1}. Although hampered by overlapping spectra, Poindexter *et al.* were able to show that the P_{b0} g tensor was virtually identical to that of the (111) Si/SiO₂ P_b; they obtained $g_\parallel = g_3 = 2.0015$ and $g_\perp \cong g_1 \cong g_2$, with $g_1 = 2.0087$ and $g_2 = 2.0080$. This very close correspondence
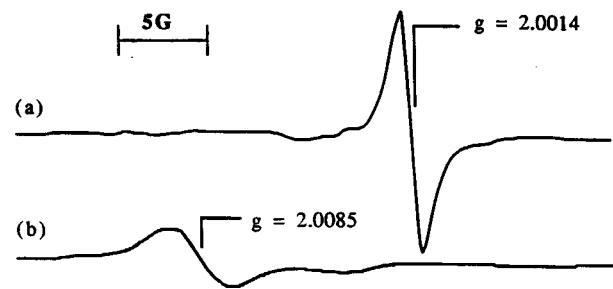

FIG. 5. EPR traces of the P_b center for the magnetic field (a) parallel and (b) perpendicular to the (111) symmetry axis.

between the (111) P_b and (100) P_{b0} g tensors was confirmed in later observations by Kim and Lenahan.[9] Poindexter *et al.*[4,5] found that P_{b1} exhibits lower symmetry: $g_1 = 2.0076$, $g_2 = 2.0052$, and $g_3 = 2.0012$. Traces of the P_b center taken with the magnetic field parallel and perpendicular to the (111) symmetry axis are shown in Fig. 5.

The close similarity between P_b and P_{b0} g tensors lead Poindexter *et al.* to suggest that the two centers are essentially identical: silicon "dangling bond" defects in which the unpaired electron resides on a silicon backbonded to three other silicon atoms at the Si/SiO₂ boundary. This identification makes physical sense: a silicon dangling bond defect *should* have a g tensor with (111) axial symmetry. [Silicon bonds point in (111) directions.] Also, as pointed out by Caplan, Poindexter and co-workers, the g tensors are consistent with those of other silicon dangling bond centers.[4] For a (111) Si/SiO₂ interface this g tensor symmetry axis should be normal to the interface (it is). Serious doubts about the basic structure of the (111) P_b and (100) P_{b0} centers should have been resolved by measurements of the hyperfine interactions with ²⁹Si nuclei. The (111) P_b hyperfine tensor was first measured by Brower[22] who found $A_\parallel \cong 152$ G and $A_\perp \cong 89$ G. The similar (100) P_{b0} hyperfine tensor was first measured by Jupina and Lenahan[23] in radiation damage studies and later by Gabrys and Lenahan[24] in hot carrier damaged transistors and (probably) quite recently by Cantin *et al.*[25] in porous silicon films. Brower's (111) results have also been confirmed by Jupina and Lenahan[23] and (probably) Cantin *et al.*[25] In all cases, the approximately 5%/95% ratio of side (²⁹Si) peaks to center (²⁹Si) peaks was reported. The $\cong 5\%$/95% ratio of "hyperfine lines" to center line intensity for both (111) P_b and (100) P_{b0} *unequivocally* establishes that both centers are *silicon* dangling bonds. The (111) P_b and (100) P_{b0} have nearly identical hyperfine tensors which demonstrate, as had been indicated by earlier g tensor results, that P_b and P_{b0} are essentially identical defects. [Of course quite subtle differences *inevitably* exist; the (111) P_b center's unpaired electron is in an orbital directed along the (111) surface normal.] The (100) P_{b0} is also directed along a (111) direction but this direction is obviously not normal to the (100) surface. The structures of the (111) P_b and the (100) P_{b0} are shown in Figs. 6 and 7.

The *detailed* structure of the P_{b1} center remains something of a mystery; although it too is clearly a silicon "dan-
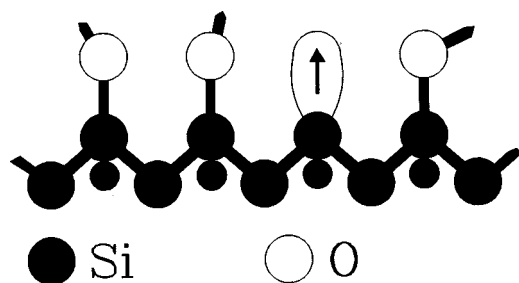
FIG. 6. Schematic illustration of a P_b center at the (111) Si/SiO$_2$ interface.

gling bond'' at the interface. Brower observed the P_{b1} ^{29}Si hyperfine interactions for a single orientation.[26] His results clearly indicate an unpaired electron localized on a silicon atom in an orbital of high p character. Brower observed P_{b1} (as well as P_{b0} and P_b) in oxides grown on both (111) and (100) silicon substrates in a ^{17}O enriched atmosphere. Since ^{17}O possesses a nuclear magnetic moment, if the P_b center silicon were bonded to an oxygen, the ^{17}O nuclear moment would greatly broaden the spectrum. None of the three P_b variants is broadened enough to indicate nearest neighbor oxygens. However, *all* are slightly broadened, indicating that they are *all at the interface*. Since nitrogen and hydrogen also possess magnetic moments we know that the P_{b0} and P_{b1} silicons could not be bonded to them either. Since no other atoms are consistently present in numbers sufficient to account for the P_b centers we may conclude that *all* three varieties of P_b center are silicons back bonded to silicons at the respective Si/SiO$_2$ boundaries.

It should be noted that Stathis and Dori[18] strenuously object to the conclusions above regarding both the structure of P_{b0} and its close similarity to the (111) P_b. They argue that ''the defect responsible for the P_{b0} resonance either is fundamentally different from a dangling bond, or lies deeper inside the silicon away from the interface.'' They also argue that ''the structure of P_{b1} is a silicon dangling bond similar to the P_b on (111) and that P_{b0} is a *fundamentally* different defect.''

Stathis and Dori[18] draw these conclusions from an experiment for which they reported on two oxide samples—one grown on a (111) surface and one on a (100) surface. The oxides were exposed to a post oxidation anneal in argon at 700 °C in a sealed oxygen free silicide anneal furnace (SAF). The (111) samples received 5 min anneals, the (100) samples
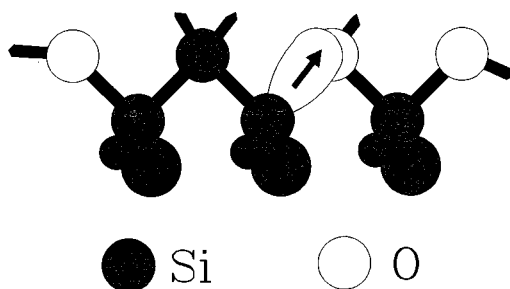
received 30 min anneals. After the anneal in the SAF both samples were placed in a furnace in an argon ambient at 760 °C and then pulled out after 30 s. Some samples received a blanket aluminum deposition after the annealing steps ''to ensure that these samples saw the same processing sequence as similar samples that were used for electrical characterization.'' (Stathis and Dori did not discuss these electrical characterizations.)

The Stathis/Dori conclusions with regard to P_{b0} not being a dangling bond, for example, apparently arise from differences they observed in the P_b, P_{b0}, and P_{b1} responses to the growth and annealing steps which were themselves somewhat different for the two samples. What conclusions may be drawn from the Stathis/Dori work are not obvious. However, in view of the enormous amount of consistent and mutually corroborating evidence generated by many other groups investigating a vastly wider range of oxides, one must conclude that the overwhelming preponderance of evidence indicating that the (111) P_b and (100) P_{b0} are virtually identical defects is convincing. Both defects are silicon dangling bonds; in this regard the hyperfine results are utterly conclusive. Both involve silicons backbonded to three other silicons and both are at the Si/SiO$_2$ boundary.

B. Electronic levels of P_b centers

Several measurements of the population of paramagnetic P_b density versus Si/SiO$_2$ interface Fermi level provide approximate but unequivocal information about the center's electronic density of states.

The first attempt at this measurement by Poindexter and co-workers[27] was not successful. They were able to show that the P_b center spin lattice relaxation time was gate bias dependent but were unable to determine whether or not the charge state is also bias dependent. (The spin lattice relaxation time is the time it takes for an electron ''flipped'' via EPR to return to its previous orientation in the magnetic field.)

Another attempt at this measurement by Brunstrom and Svenson,[28] although qualitative in nature, showed that the application of a very large positive or negative bias across the oxide could suppress much of the P_b amplitude. From this observation, Brunstrom and Svenson inferred that P_b centers can accept both electrons and holes.

The first *semiquantitative* and *quantitative* information about P_b levels within the Si band gap was reported by Lenahan and Dressendorfer[7,8] who measured the ESR amplitude of the unsaturated P_b absorption spectra as a function of the interface Fermi level using a TE$_{104}$ double resonant cavity and a calibrated spin standard. Their results are shown in Fig. 8. Investigating irradiated thermal oxides, they found that the distribution of P_b centers is broadly peaked. Below mid-gap the P_b center is a donorlike interface state defect ($P_b = P_b^+ + e$; $P_b + h^+ = P_b^+$). As the Fermi level moves toward mid-gap, the positively charged P_b center accepts an electron and becomes paramagnetic and neutral ($P_b^+ + e^- = P_b$). As the Fermi level moves from mid-gap to the conduction band edge, the P_b center picks up another electron,
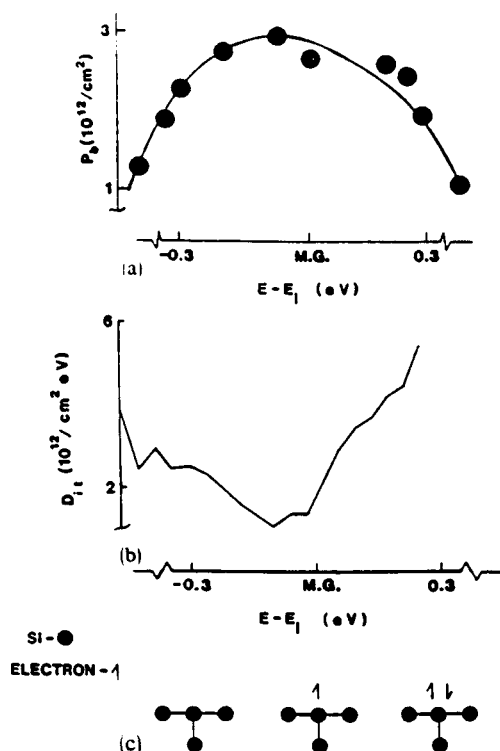

FIG. 7. Schematic illustration of a P_{b0} center at the (100) Si/SiO$_2$ interface.

FIG. 8. (a) Population of paramagnetic P_b centers vs the position of the Fermi energy at the Si/SiO$_2$ boundary (b) Density of interface states. (c) Schematic illustration of P_b occupation vs Fermi energy.

becoming negatively charged and again diamagnetic. In the upper part of the band gap, the P_b center is thus an acceptorlike interface trap ($P_b + e^- = P_b^-$; $P_b^- + h^+ = P_b$). The P_b center is paramagnetic when it has an unpaired (one) electron; it becomes diamagnetic by either accepting or donating an electron. The distribution of paramagnetic P_b centers is consistent with the ''U-shaped'' distribution of interface traps that is generally reported. Lenahan and Dressendorfer proposed that the P_b density of states could be roughly approximated by the absolute value of the derivative of the P_b versus energy curve, yielding a U-shaped distribution. The spin state of the P_b center corresponding to its rough position in the gap is also displayed in Fig. 8.

Lenahan and Dressendorfer's results showed that P_b centers are amphoteric: P_b centers are positively charged and diamagnetic when the Fermi level is near the valence band and negatively charged and diamagnetic when the Fermi level is near the conduction band. When the Fermi level is near the center of the gap, P_b centers are paramagnetic and have no net charge.

Lenahan and Dressendorfer pointed out that if P_b centers account for most of the interface traps, then one can separate the effects of oxide space charge from interface charge by measuring capacitance versus voltage shifts corresponding to the Fermi level at mid-gap, where the P_b centers are electrically neutral.

Poindexter et al.[29] subsequently confirmed this P_b versus energy result. They published an essentially identical energy distribution plot for P_b in unirradiated high temperature as

processed oxides. A recent study by Semon and Lenahan[28] also confirms the original results; they found that the distribution of P_b centers in a wide variety of oxides is roughly the same and that the electron–electron correlation energy of the P_b is about 0.7 eV. Gerardi et al.[30] established that the energy levels and correlation energy for P_{b0} are nearly identical to the P_b (111). They also report that the P_{b1} has a smaller correlation energy than the P_{b0} and a distribution skewed towards the top of the gap. Kim and Lenahan[9] later obtained P_{b0} versus Fermi energy results nearly identical to those off Gerardi et al.; they also showed that the P_{b0} center (and not the P_{b1}) is primarily responsible for ^{60}Co radiation induced interface traps (D_{it}).

Although Lenahan and Dressendorfer and the Poindexter group published virtually identical P_b amplitude versus energy curves, they interpreted them in slightly different ways. Whereas Lenahan and Dressendorfer proposed that the absolute value of the derivative of P_b amplitude versus energy $|dP_b/dE|$ would *roughly* correspond to the P_b density of states, Poindexter et al. presented a plot of $|dP_b/dE|$ *as* the density of states. Although Poindexter et al. also clearly viewed this as an approximation, the idea that $|dP_b/dE|$ represents the P_b density of states has caused some misunderstandings. The $|dP_b/dE|$ curve goes to zero near mid-gap; if $|dP_b/dE|$ very accurately represented the P_b density of states, there would be zero P_b levels at mid-gap. It is clear that this is not the case from at least two types of measurements: (1) spin dependent recombination studies of irradiated and hot carrier stressed metal–oxide–semiconductor field-effect transistors (MOSFETs) and (2) a comparison of mid-gap interface state densities and P_b densities in many as processed (and relatively poor) Si/SiO$_2$ samples.

In spin dependent recombination (SDR)[31] one detects EPR via spin dependent changes in a recombination current in a semiconductor device. SDR was discovered by Lepine,[31] who showed that the spin dependent capture of charge carriers at paramagnetic deep levels could be modulated via EPR and that EPR induced changes in capture probability could be measured in a recombination current. Lepine proposed a very simple model which, although not completely correct, provides qualitative understanding. A strong applied magnetic field polarizes the spins of both the paramagnetic trapping centers and the paramagnetic charge carriers. With both trap and charge carrier spin systems polarized, imagine the capture of an electron at a P_b center dangling bond site. If both the P_b center and conduction electron spin point in the same direction, the recombination event will be forbidden. Thus, the application of a large magnetic field will reduce charge carrier capture and thus will also reduce a recombination current. However, in EPR, the application of a microwave frequency field satisfying the resonance condition will ''flip'' the trap electron. The trapping event is no longer forbidden and the recombination current increases. Thus, by measuring the recombination current versus applied field while simultaneously applying microwave radiation, one may identify the defects dominating recombination. The current versus field SDR spectrum will almost exactly match the
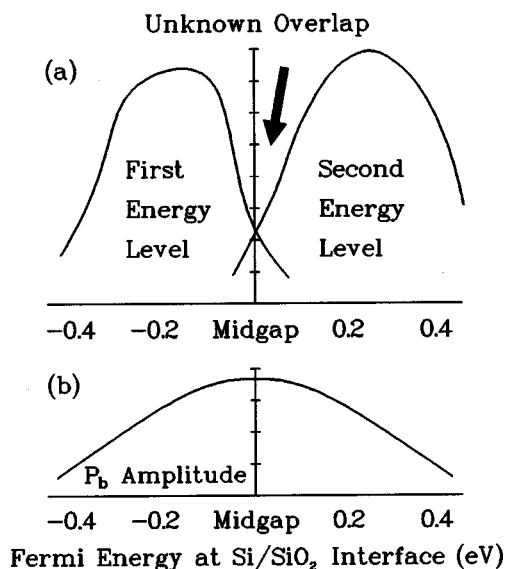
FIG. 9. Schematic density of states for P_b centers.

EPR spectrum of the defect (or defects) involved in recombination.

Grove, Fitzgerald, and co-workers[32-34] extensively investigated recombination currents in gate controlled MOS diodes. They showed that near mid-gap interface states are almost entirely responsible for recombination currents when these devices are biased to yield the maximum recombination current. Both the pioneering SDR study of Vranch et al.[10] and the later more extensive SDR measurements of Jupina and Lenahan[23] reported quite strong P_b SDR spectra under these biasing conditions, results essentially impossible to reconcile with a near zero P_b density of states in the vicinity of mid-gap.

Almost equally compelling objections to the notion of near zero P_b density at mid-gap come from an examination of the early collaboration between Caplan, Poindexter, Deal and Razouk (CPDR).[4,5] In the CPDR studies P_b and mid-gap interface state densities were evaluated on a variety of as-processed Si/SiO₂ samples with relatively high mid-gap interface state densities in the range of $\sim 1 \times 10^{11}/cm^2$ eV to $2 \times 10^{12}/cm^2$ eV. (CPDR reported a virtually one-to-one correlation between the P_b densities and 1 eV times the mid-gap interface state densities.) If the P_b density of states were virtually zero, Poindexter et al. could not have obtained the results they reported. (Obviously, if the P_b densities at mid-gap were very low, the mid-gap interface trap density $/P_b$ density ratio *has* to be very high.)

A schematic illustration of the P_b density of states is shown in Fig. 9. As recently demonstrated for P_b-like dangling bonds in amorphous hydrogenated silicon,[35] this schematic curve should be viewed as exactly that—a *schematic*. The shape of the density of states curve will depend to some extent upon the density of P_b centers.[35] The P_b energy levels couple to the band tail states which they themselves (in part) create. P_b defects close to one another will have a coupling between their own levels.[35] Nevertheless the schematic illustration is a reasonable zero order description of P_b levels.

Two broad levels separated by a correlation energy of ~0.6 eV; a quite significant P_b density of states exists at mid-gap.

VI. ROLE OF P_b IN Si/SiO₂ INTERFACE INSTABILITIES

The Si/SiO₂ interface can be damaged when MOS devices are stressed in a variety of ways. Among the stressing phenomena, ionizing radiation has been the most extensively investigated, although a considerable body of work also exists regarding hot carrier and high electric field effects.

A. Radiation damage

Several early studies by Lenahan, Dressendorfer et al.[6-8,36] using (111) Si/SiO₂ structures, established that when MOS devices are subjected to ionizing radiation, P_b centers are generated in densities which approximately match the average of the interface state densities generated in the mid-half band gap. They showed that the annealing characteristics of the P_b centers and radiation induced interface state densities are virtually identical. They furthermore demonstrated that the densities of radiation induced P_b centers could be strongly influenced by processing variations. Processing yielding low P_b generation also produced low yields of radiation induced interface state densities. Processing yielding higher P_b densities resulted in proportionately larger interface state densities. A later study by Kim and Lenahan[9] extended these results to the more technologically important (100) Si/SiO₂ system. Some results from these studies are shown in Figs. 10 and 11. As mentioned previously, an interesting aspect of the Kim/Lenahan study was the observation that the radiation induced P_b centers were primarily (although not exclusively) P_{b0} defects. (Weaker P_{b1} spectra were also generated.) The results of these studies have been confirmed and extended by many other groups.

Miki et al.[11] compared the response of ultradry and steam grown oxides to ionizing radiation. They found higher densities of radiation induced interface states and higher densities of radiation induced P_b centers in the steam grown oxides. They also found a rough numerical correspondence between the ratios of induced P_b and interface state defects as well as in the absolute numbers of P_b centers and interface states. However since the EPR measurements were made on soft x-ray irradiated devices and the electrical measurements were made on devices in which holes were avalanche active injected into the oxide (to simulate the radiation) precise numerical comparisons were not possible.

Awazu et al.[12] have also studied the role of processing parameters on the generation of P_b centers by ionizing radiation. Among the oxide processing parameters investigated were those used in the first study of Lenahan and Dressedorfer. For these oxides, Awazu et al. obtained the same P_b versus dose curve reported in the original 1981 study.

Awazu et al.[12] studied oxides grown on both (111) and (100) substrates. They found that if an as-processed interface had low P_b density then technologically relevant irradiation levels (<10 Mrad) generated very large ($\sim 10^{12}/cm^2$) P_b
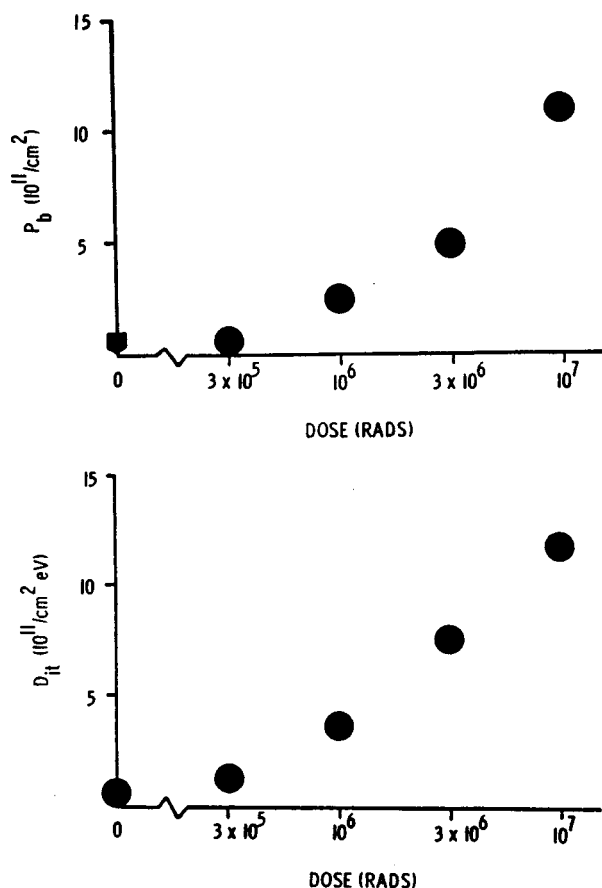
FIG. 10. Plot of P_b density (above) and interface state density in the mid-half band gap as a function of ionizing radiation dose.
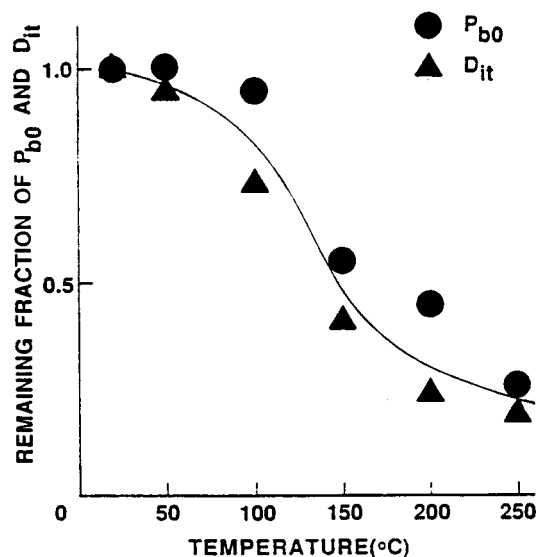

FIG. 11. Plot of the annealing behavior of P_b centers and the interface state density in the middle half of the silicon band gap vs ionizing radiation dose.

densities. However, if the as-processed P_b densities were extremely high ($\sim 2-3 \times 10^{12}/cm^2$) the P_b density was reduced. They argued that this result should be expected from elementary reaction theory.

Vranch et al.[10] have also investigated the effects of ionizing radiation on the silicon–silicon dioxide. They showed that dose levels of several megarad could generate $\sim 10^{13}$ P_b centers/cm² as measured in a conventional EPR measurement. Their studies included conventional EPR as well as spin dependent recombination. They found (as did several other groups) a strong preponderance of P_{b0} centers generated by radiation stressing.

B. High and low oxide field electron injection

In addition to ionizing radiation, several other oxide stressing mechanisms have been investigated by EPR. Mikawa and Lenahan[37] found that P_b centers could be generated by injecting electrons into an oxide at low field by internal photoemission. Warren and Lenahan[38] showed that P_b centers could also be generated by high field stressing oxides. In both the Mikawa/Lenahan and Warren/Lenahan studies a rough (about one to one) correspondence was observed between the densities of P_b centers generated and the densities of interface states in the middle half of the band gap.

C. Hot carrier stress of short channel MOSFETs

Krick et al.[39] and Gabrys et al.[24] have used SDR to study hot carrier damage centers created near the drain of short channel MOSFETs. To the best of our knowledge, these studies included the highest sensitivity electron spin resonance measurements ever made in condensed matter. Both Krick et al. and Gabrys et al. generated strong P_b SDR signals by hot hole stressing the drain regions of the transistors. Krick et al. reported that the P_{b0} SDR signal scaled with increasing interface state density as measured by charge pumping. The Gabrys measurements were sufficiently sensitive to allow detection of the ^{29}Si hyperfine side peaks as well as an evaluation of the P_{b0} ^{29}Si hyperfine tensor.

D. Conclusion regarding P_b centers and Si/SiO₂ instabilities

At least four independent groups[6–12,23,24,37–39] have reported essentially incontrovertible measurements on many oxides demonstrating a strong generation of P_b centers in device stressing. For radiation induced instabilities, all four groups concluded that P_b centers play a dominating role. Although these studies have been most extensive for ionizing radiation, one may reasonably conclude that P_b centers do indeed play dominating roles in several technologically important instabilities. The earlier studies of Nishi et al.[2–5] and Poindexter et al.[4,5] established that P_b centers play dominating roles in as-processed Si/SiO₂ structures with relatively poor interfaces.

E. Dissenting opinion

It should probably be noted that Cartier and Stathis[19] have strenuously objected to this conclusion. In a recent paper, they wrote that ''prior to these studies, it was widely accepted that the silicon dangling bond defect, which gives rise

to the well known P_b signal in ESR is the microscopic defect causing the fast interface states. As will be outlined in this contribution, we cannot support this view.'' They argue that ''silicon dangling bonds, as detected by ESR measurements account for only *a small* fraction of the electrically detected interface states'' (emphasis added).

Cartier and Stathis draw this conclusion on studies in which they bombard Si/SiO₂ structures with *extremely* high fluences of atomic hydrogen (up to 10^{21} hydrogen atoms/cm²) to generate extremely high densities of interface states ($>5 \times 10^{12}$/cm² eV).

There are a few problems with the Cartier/Stathis study. At least five bear mentioning.

(1) The $\approx 10^{21}$ hydrogen atoms/cm² used in their study corresponds to about *one million monolayers*. A typical oxide ~100 Å thick with ~0.1 at. % hydrogen would have about 10^{14} hydrogen atoms/cm². Thus, the amount of hydrogen involved in their model experiments is many orders of magnitude greater than that present in the process they are attempting to model.

(2) Ionizing radiation, in particular, has been well studied. Atomic hydrogen is dimerized in a fraction of a second at room temperature.[40] At room temperature, generation of interface states proceeds for *many seconds* after a device is exposed to ionizing radiation.[41,42] Since atomic hydrogen is not present during nearly all the time involved in interface state generation, atomic hydrogen by itself *cannot* be responsible for most of the process.

(3) Johnson et al.[43] have shown that atomic hydrogen is extremely effective in annihilating silicon dangling bonds. Testing a silicon dangling bond generation model with a process known to annihilate silicon dangling bonds is a less than an optimal approach.

(4) A fourth problem with the work of Cartier and Stathis involves the extremely high amounts of energy which would be required to generate fluences of 10^{21} hydrogen atoms/cm². For example, if one were actually to flood an interface with 10^{21} hydrogen atoms/cm², say via ionizing irradiation, one would necessarily have to break 10^{21} hydrogen atoms bonds/cm². If each bond energy is ~2 eV, $\sim 2 \times 10^{21}$ eV/cm² would be absorbed by the ~100 Å oxide involved. (Stathis et al. reported results of P_b generation in 97.5 Å oxides.) Radiation dose is typically reported in rads: 1 rad = 10^2 ergs/gram. For Si/SiO₂ then,

$$1 \text{ rad} = \left(10^2 \text{ erg/g}\right)\left(\frac{10^{-7}J}{\text{erg}}\right)\left(\frac{\text{eV}}{1.6 \times 10^{-19}J}\right)$$

$$\times \left(\frac{2.2 \text{ g(SiO}_2)}{\text{cm}^3}\right) \cong 1.4 \times 10^{14} \text{ eV/cm}^3.$$

Thus, for a 100 Å thick oxide, a fluence of 10^{21} hydrogen atoms/cm² would correspond to a dose of *at least* 1.3×10^{13} rad. This is about a million times higher dose level than the highest levels utilized in the earlier studies and, not coincidentally, a million times higher than the upper limit of technological relevance. Indeed, this amount of energy is orders of magnitude higher than that required to vaporize the oxide sample in question.
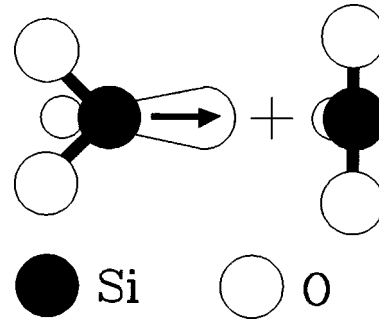

FIG. 12. Schematic illustration of the E' center.

(5) There is another, slightly more subtle problem with the Cartier et al. study. Their fundamental result, gross differences in P_b and interface state densities, involved EPR measurements of P_b centers on 97 Å oxides and capacitance versus voltage measurements on 495 Å oxides.[44] An extremely large number of studies involving radiation damage have consistently shown that interface state generation is a very strong fraction of oxide thickness.[45–47] Since very large differences in interface state generation are consistently observed for different oxide thicknesses, one would not expect a 97 Å oxide and a 495 Å oxide to exhibit comparable interface state densities in the process which Cartier et al. attempt to model. (Indeed, the thinner oxide would be expected to exhibit much lower interface state density.[45–47])

Although the Stathis/Cartier atomic hydrogen studies may be of some general interest, their conclusions are not strongly supported by their own data and are contradicted by much more relevant and extensive data generated by many other groups.

VII. OXIDE CENTERS: NEAR Si/SiO₂ CENTERS

A. E' centers structure

The most important oxide trapping centers are E' centers, which involve an unpaired electron localized on a silicon backbonded to three oxygens. Usually, though not always, the paramagnetic silicon site is coupled to a positively charged diamagnetic silicon as shown in Fig. 12.

E' centers have been studied in cubic centimeter sized samples for quite some time.[48,49] In these large volume samples, it is quite easy to measure the hyperfine interactions of the unpaired electron with the single silicon atom on which it primarily resides. Although the magnetic ²⁹Si nuclei are only ≅5% abundant, the number of centers present in large volume samples (typically $\sim 10^{16} - 10^{17}$/cm³ for amorphous SiO₂) is more than sufficient to generate quite strong ²⁹Si spectra. An EPR spectrum taken on such a large volume amorphous sample is shown in Fig. 4. As discussed previously one may, by inspection, obtain a rough estimate of the hybridization and localization of the electron from this spectrum. Also, as discussed previously, one notes that a second integration of the two side peaks (corresponding to spin 1/2
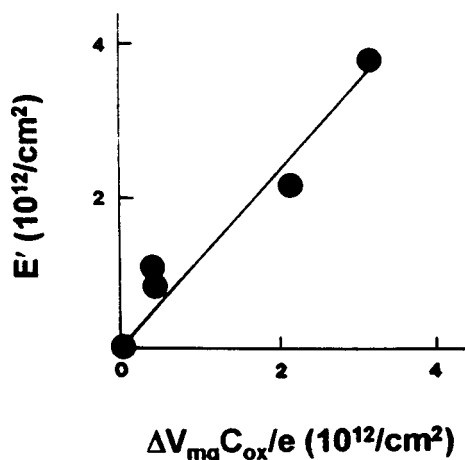
FIG. 13. Plot of E' density vs trapped hole density in MOS oxides subjected to ionizing radiation.

FIG. 14. Plot of trapped hole density and E' density vs dose for oxides irradiated under positive gate bias.

nuclei) yields an intensity of about 5% of the center line—unambiguously identifying the center as an unpaired spin localized on a silicon atom.

In crystalline SiO_2, Feigl et al.[49] argued that E' centers are holes trapped in oxygen vacancies. The unpaired electron resides on a neutral silicon on one side of the vacancy. The silicon on the other side of the vacancy is positively charged. Bonded to just three other atoms, it adjusts its position to a flat-planar arrangement (expected for sp^2 bonding) with its three neighboring oxygens. In amorphous SiO_2, E' centers can be positively charged or neutral.

Quite a number of studies indicate that E' centers are dominating trapped hole centers in technologically relevant thermally grown oxide films.[8,9,11–16,36,50] These E' centers are primarily the positively charged Feigl Fowler Yip E' defects shown in Fig. 12.

B. MOS oxide E' centers: Electronic properties

The role of E' centers in high quality thermally grown oxides is fairly well understood at the present time. These centers were probably first detected in thermally grown oxides by Marquardt and Sigel[51] who studied quite thick (up to 11 000 Å) oxides subjected to quite high (up to 220 Mrad) doses of ionizing radiation. They observed weak signals in these films which they attributed to E' centers. Although they did not report results of electrical measurements, they proposed (correctly) that E' centers are thermal oxide hole traps.

The electronic properties of E' centers and their significance in MOS device operation were first demonstrated by Lenahan and Dressendorfer.[8,36] They made a series of observations which clearly established that E' centers are dominating hole trap centers in a variety of MOS oxides. (1) They found a rough one-to-one correspondence between E' density and the density of hole traps in relatively hard and relatively soft oxides grown in both steam and dry oxygen (see Fig. 13). (2) They found a rough one-to-one correspondence between E' density and trapped hole density in oxides irradiated under positive gate bias over a technologically mean-
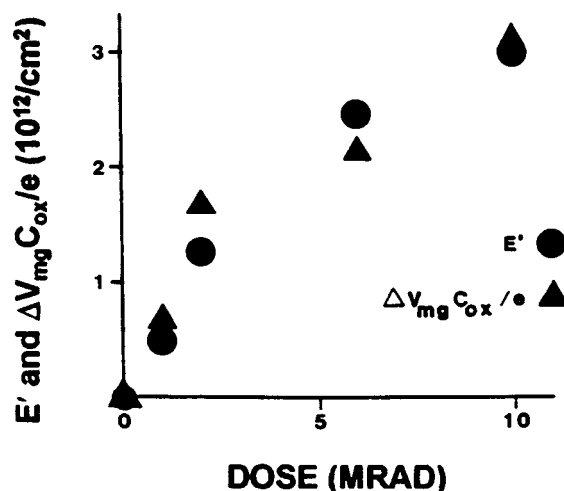
ingful range of ionizing radiation dose (see Fig. 14). (3) They showed that MOS oxide E' centers and oxide trapped holes have the same annealing response in air (see Fig. 15). (4) They demonstrated that the distribution of E' centers and trapped holes are virtually identical in oxides subjected to ionizing irradiation under positive gate bias: both the trapped holes and E' centers are quite close to the Si/SiO_2 boundary (see Fig. 16).

The results of the early studies have been confirmed and extended in quite a few later studies. (1) Takahashi and co-workers[52,53] also reported an approximately one-to-one correspondence between E' centers and trapped holes; they also reported that the distribution of E' centers and trapped holes were the same in their irradiated oxides. (2) Lipkin
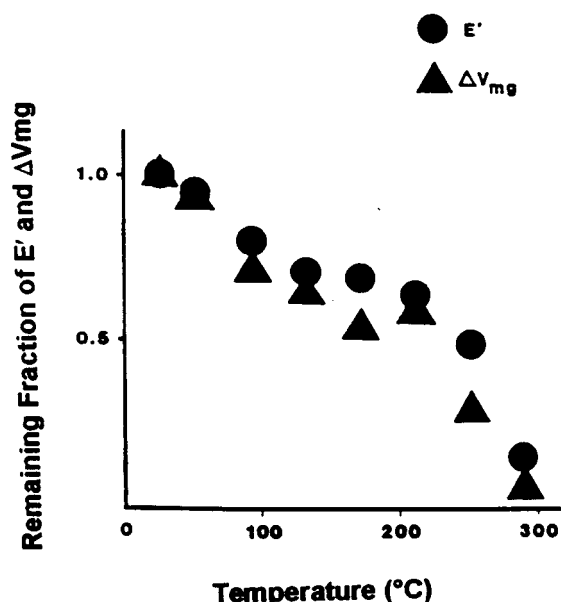

FIG. 15. Annealing response of E' centers and holes trapped in the oxide.
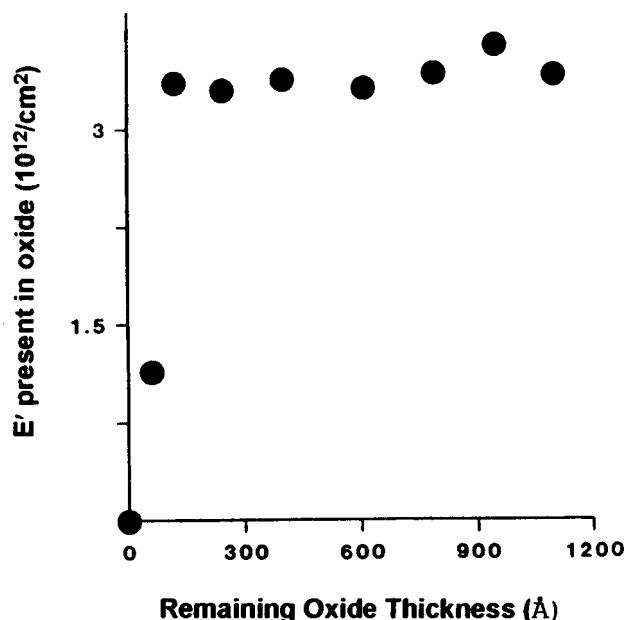
FIG. 16. Plot of E' centers remaining in an oxide after a series of etch back steps. The results show that nearly all the E' centers, like nearly all the trapped holes, are near the Si/SiO₂ boundary.

et al.[54] also measured an approximately one-to-one correspondence between E' density and the density of trapped holes generated in oxides subjected to 10–20 Mrad of gamma radiation (3) Miki et al.[11] compared both E' generation and trapped hole generation in ultradry and steam grown oxides. They found that their ultradry oxides contained twice as many E' centers as the steam grown oxides and that the ultradry oxides also had twice as many trapped holes as the steam grown oxides. In addition, they found a rough numerical correspondence between the E' densities and trapped hole densities in the samples investigated. However, since Miki et al.[11] made electrical measurements on oxides subjected to avalanche injection of holes and EPR measurements on x-ray irradiated oxides, a precise numerical comparison between E' density and trapped hole density was not possible. (4) Awazu et al.[12] have explored the role of processing parameters on E' generation. As previously noted by Lenahan and Dressendorfer,[8,36] as well as by Miki et al.,[11] the densities of E' centers are strongly processing dependent. A point of particular interest in the Awazu study is their observation that the cooling rate after high temperature processing strongly affects E' generation. Awazu et al. concluded that the E' centers in their oxides were holes trapped in oxygen vacancies $O_3 \equiv Si + \cdot Si \equiv O_3$. Since they observed $\sim 1-3 \times 10^{12} E'$ centers/cm² after modest ($\sim 1-11$ Mrad) doses of ionizing radiation, these centers would inevitably be the dominant hole trap centers in the oxides of their study. (5) Results of a more qualitative nature by Carlos[14] also support the correspondence between oxide trapped holes and E' centers. He reported a significant ($\sim 10^{12}$/cm²) density of E' centers in oxides subjected to technologically relevant radiation levels. Although he did not report results of any electrical measurements, he did report a gate polarity dependence

of E' generation, suggesting (as the other studies had shown) that E' generation was due to the capture of a charged particle.

The results of at least five independent EPR studies all indicate a dominant role for E' centers in oxide hole trapping. On the basis of this mutually corroborating work we conclude that E' centers do indeed dominate oxide hole trapping in a wide variety of thermally grown oxide films on silicon. However, the current understanding of oxide hole trapping is moderately complex and still incomplete. At least five E' variants have been observed in thermally grown oxide films. Two E' variants are E' defect/hydrogen complexes for which detailed and convincing models have yet to be established. A third variant called E'_δ or EP is almost certainly closely related to the conventional E' site but exhibits significantly different g and hyperfine tensor components and somewhat different capture cross sections than the conventional E' site. A fourth variant, called EP2 is even less well characterized. It is positively charged when paramagnetic and exhibits a large capture cross section for holes. A fifth variant is the neutral E' center, observed in plasma-enhanced chemical vapor deposition (PECVD) oxide films and in thermally grown oxides exposed to very high doses of ionizing radiation.

VIII. HYDROGEN COMPLEXED E' CENTERS

Two hydrogen complexed E' variants may play important roles in device reliability. The hydrogen complexed centers are called the 74 G doublet and the 10.4 G doublet. EPR traces of both defects are shown in Fig. 17. Both defects were first observed in cubic centimeter size samples,[55,56] and both centers clearly involve an E' hydrogen complex. It has been proposed[55] that the 74 G doubled involves an unpaired electron on a silicon back bonded to two oxygens and one hydrogen and that the 10.4 G doublet defect involves an unpaired electron on a silicon back bonded to three oxygens with one of the oxygens bonded to a hydrogen.[55] (Although these models seem quite reasonable and are undoubtedly correct to the extent that the defects are E'/hydrogen complexes, in detail, the models should probably be viewed as provisional.)

The 74 G doublet was first observed in thin oxide films by Takahashi et al.[52,53] who generated them at somewhat elevated temperatures ($\cong 100$ °C) in irradiated oxides. More recently, Conley et al.[57,58] observed the room temperature generation of both the 74 G doublet centers and 10.4 G doublet centers in oxides subjected to either vacuum ultraviolet ($hc/\lambda \leq 10.2$ eV) or gamma irradiation.

Takahashi et al.[52,53] suggested that the hydrogen complexed E' defects might play an important role in Si/SiO₂ interface state generation. Conley et al.[57,58] provided strong circumstantial evidence linking E'/hydrogen coupled centers to interface trap generation. Several (purely electrical measurement) studies[59,60] had shown that a molecular–hydrogen-containing ambient leads to an enhancement in radiation induced interface state generation. Conley et al.[57,58] showed that exposing an oxide previously flooded with holes (to gen-
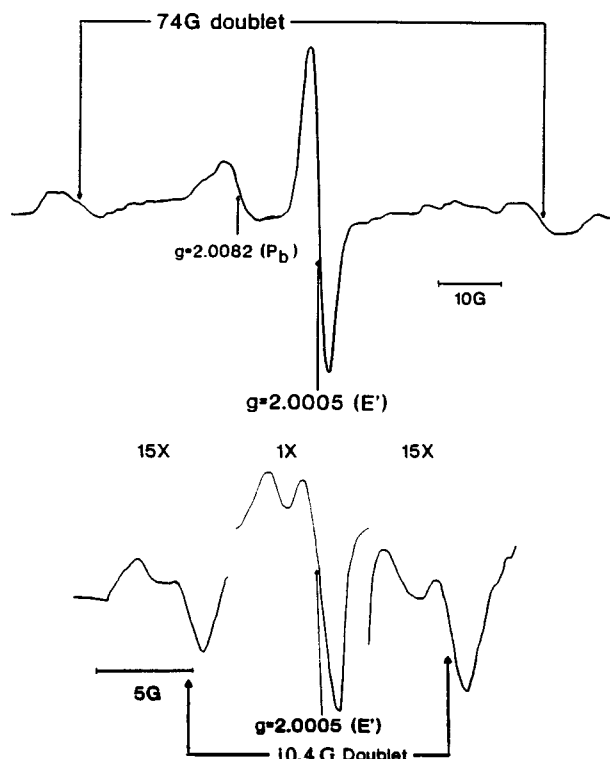
FIG. 17. EPR traces of (a) the 74 G doublet and (b) the 10-4 G doublet centers.

erate E' centers) to an H$_2$/N$_2$ ambient leads to a conversion of conventional E' centers to 74 G doublet centers as well as generation of interface state centers. The number of E' centers converted to hydrogen complexed centers is approximately equal to the number of interface traps generated. The time period involved in interface trap formation is approximately equal to the time required to saturate the E'/hydrogen complexing process.

IX. EP OR E'_δ VARIANT (ONE DEFECT, TWO NAMES)

The EP or E'_δ variant has been observed in separation by implanted oxide (SIMOX) buried oxides,[61–65] bond and etch back (BESOI) buried oxides, and thermally grown oxides. It is generally observed simultaneously with the conventional E' center. Its spectrum is quite narrow with a zero crossing $g \cong 2.002$. Vanheusden and Stesmans[64] estimate that the E'_δ/EP variant accounts for about 20% of the E' centers in SIMOX buried oxides. Conley et al.[61,63,65,66] have observed EP/E'_δ centers in a variety of thermally grown oxides as well as in SIMOX buried oxides and demonstrated that they are positively charged.

Vanheusden and Stesmans and Warren et al.[63] had initially proposed that the EP/E'_δ center involved a five silicon atom microcluster. Conley and Lenahan[67] compared the response of the EP/E'_δ centers to molecular hydrogen and found nearly identical responses for both centers: virtually identical time scales for the room temperature response, nearly identical hyperfine coupling constants for both hydro-

gen complexed centers, and nearly identical g values for both hydrogen complexed centers. On the basis of those observations, they argued that the EP/E'_δ center must be very closely related to conventional E' centers, and almost certainly not a five atom silicon cluster. Recent studies of the EP/E'_δ ^{29}Si hyperfine spectrum indicated that the unpaired electron is shared by two equivalent silicons.[67]

Quite recently, Chavez et al. have proposed that the EP/E'_δ center is an oxygen vacancy but with the positive charge and the unpaired electron equally shared by the two silicons. The model proposed by Chavez et al.[68] is consistent with many experimental observations: (1) as observed experimentally, the center is positively charged, (2) as observed experimentally the center behaves almost exactly like the conventional E' center in response to molecular hydrogen. (3) The predicted hyperfine coupling is almost exactly what is observed experimentally. (4) The model is consistent with recent observations indicating that the unpaired electron is shared by two silicons. There is extensive agreement between the Chavez model and experimental observations; it's probably correct.

X. NEAR Si/SiO$_2$ INTERFACE E' CENTERS: ELECTRONIC PROPERTIES

One could reasonably divide electrically active MOS defects into three categories: Interface state traps, which can communicate readily with charge carries in the silicon, oxide traps which do not communicate with charge in the silicon, and very near interface traps which can, on fairly long time scales, communicate with charge carriers in the silicon.

The near Si/SiO$_2$ interface traps go by many names: slow states, border traps, switching traps,... . It is possible, even likely, that more than one type of near Si/SiO$_2$ interface trap can exist in certain oxides under certain conditions. One near Si/SiO$_2$ interface trap has been directly identified via EPR the E' center.

Many studies (involving only electrical measurements) show that when some MOS devices are subjected to ionizing radiation capacitance versus voltage and current versus voltage, characteristics experience a negative voltage shift, ΔV, indicating the capture of positive charge in the oxide.[69,70] However, if a positive gate bias is applied, the magnitude of ΔV decreases logarithmically in time, indicating the annihilation of some of the positive charge. If the applied bias is reversed from positive to negative some of the previously annihilated charge returns. The charge that returns is said to be in switching traps.

An EPR study by Conley et al.[71] clearly demonstrates that some E' centers can act as switching traps. These centers are presumably very close to the Si/SiO$_2$ boundary. Results from the Conley et al.[71] study are shown in Fig. 18. The bias voltages and bias switching times approximately match those of earlier purely electronic measurements. The first point (HOLES) indicates the E' density initially after holes were injected into the oxide. The second point (Zero 1) was taken after 10^5 s with no bias across the oxide. Point (Neg 1) was taken after a negative gate voltage corresponding to an aver-
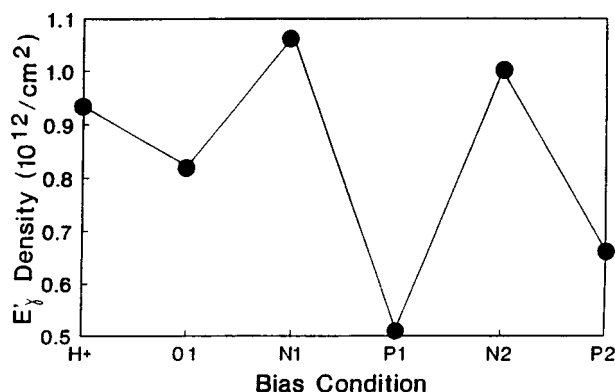
FIG. 18. Plot of E' spectrum amplitude vs the biasing sequence discussed in the text.

age oxide field of 3.5 MV/cm was applied for 24 h. The negative bias increased the number of paramagnetic E' sites. Point (POS 1) was taken on the same sample after an additional 24 h under positive gate bias, also corresponding to an average oxide field of 3.5 MV/cm. The positive bias substantially decreases the density of paramagnetic E' centers. Two additional biasing points indicate the repeatability of this process. Clearly, the ''spin state'' and thus ''charge state'' of these E' centers can be repeatably switched with bias;thus E' centers can act as oxide switching traps.

The results of Conley *et al.*[71] are consistent with, and clearly confirm, the basic premise of the switching trap model proposed earlier by Lelis *et al.*[69,70] after hole capture, subsequent electron capture does not always return the E' site involved to its original condition. This irreversibility leads to the switching behavior. The results of Conley *et al.* do not, of course, preclude the possibility that defects other than E' centers may act as switching traps.

The Conley *et al.*[71] results extend earlier results generated by Jupina and Lenahan who reported the SDR detection of E' centers.[21] Since SDR can only detect defects which in some way ''communicate'' with Si/SiO$_2$ interface charge carriers, their results strongly indicated that some near Si/SiO$_2$ interface E' centers did indeed behave in this way. The Conley *et al.* study is also consistent with a recent ESR study by Warren *et al.*[72] which suggested, but did not demonstrate, that E' centers may act as switching traps.

XI. INTRINSIC DEFECTS AND DEVICE RELIABILITY: PHYSICALLY BASED PREDICTIVE MODELS

Although the many EPR studies of MOS systems are of some general interest as physics, chemistry, and materials science, their ultimate significance must relate to their utility: can these studies help design better, more reliable, integrated circuits? The answer to this question is almost certainly yes. Yes, if the results can be utilized to predict and manipulate defect densities.

It is clear that two families of point defects, E' centers and P_b centers, play dominating roles in a number of MOS reliability problems. Materials scientists and engineers have

well developed and widely verified methods of manipulating intrinsic point defect populations. These methods are based upon the fundamental principles of the statistical mechanics of solids as well as on basic principles of physical chemistry.

One should be able to ameliorate device reliability problems by applying these well established principles to E' and P_b centers.

A. Predicting oxide hole trapping

Lenahan and Conley[15] used the standard approach of statistical mechanics[73,74] to calculate the density of oxygen vacancies in MOSFET oxides, calibrated the parameters of the expression with EPR measurements, and then tested the validity of calibrated (quantitative) expression on several oxide films. They found good correspondence between the calibrated expression and experimental results.

A consideration of the basic principles of statistical thermodynamics tells us that equilibrium occurs when the Gibbs free energy G of a solid is minimized.[73,74] It can be shown that, for the simplest cases, the minimization of Gibbs free energy leads to an equilibrium density of vacancy sites given by

$$n = N e^{\Delta S_f/k - \Delta H_f/kT}, \tag{13}$$

where ΔS_f represents the nonconfigurational entropy contribution per defect site, ΔH_f represents the enthalpy of formation of a defect site, k is the Boltzmann constant, and N represents the density of available sites. For the purposes of this discussion, the important points here are that the nonconfigurational entropy contribution is large and essentially temperature independent, and the ΔH_f essentially represents the increase in system energy caused by vacancy creation of an unstressed lattice site minus the strain energy lost by removal from a compressed SiO$_2$ matrix. (This reduction in ΔH_f would be a strain energy $\sim PdV$ caused by the effective volume change resulting from the removal of the atom from its particular location.)

As pointed out by Ohmameuda *et al.*[75] this strain energy reduction will be greatest for sites near the Si/SiO$_2$ boundary; this energy contribution should amount to several tenths of an electron volt.[6] One thus expects and finds[8] that the E' centers are primarily located close to the Si/SiO$_2$ boundary.

Anticipating then an oxygen vacancy/E' precursor density of the form

$$n = \alpha e^{-\beta/T}, \tag{14}$$

where the temperature independent constant α is given by $\alpha = N e^{\Delta S_f/k}$ and $\beta = \Delta H_f/k$, we may evaluate the relevant ''thermodynamic'' constants by making measurements on devices exposed to various high-temperature anneals. With a knowledge of E' center hole capture cross section[14] and the standard analysis of charge capture in oxide films, we would anticipate that, for a given fluence of holes through the oxides,

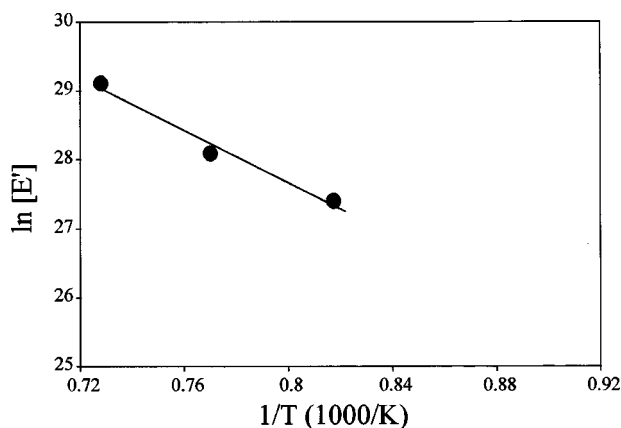$$N_{th} = \alpha e^{-\beta/T}(1 - e^{-\sigma \eta}), \tag{15}$$

FIG. 19. Plot of the natural logarithm of E' density vs the reciprocal of annealing temperature. Slope of the line yields an activation energy of to be about 1.5 eV.

FIG. 20. Solid lines represent Eq. (16) evaluated for the various indicated temperatures. Dots represent experimental results.

where N_{th} is the density of trapped holes and η is the fluence of holes through the oxide. With α, β, and σ evaluated from spin resonance measurements the expression provides a no-adjustable-parameter prediction of oxide hole trapping. (However, due to the modest absolute precision of EPR measurements, the value of α as determined strictly from EPR could be in error by almost a factor of 2.)

The potential validity of Eq. (15) was assessed[15] through a series of measurements on MOS oxides subjected to anneals at 875, 950, 1025, and 1100 °C. The oxides were all grown at 825 °C and then a polysilicon gate was deposited. After gate deposition the anneals were carried out for 30 min in a dry N$_2$ atmosphere. After the anneals the capacitors were rapidly pulled from the furnace in order to ''quench in'' the defect densities at the annealing temperatures.

The poly gates were removed and two sets of measurements were made on the samples, both after subjecting the oxides to hole flooding. To evaluate the E' precursor enthalpy of creation, oxides of the three higher temperature annealing samples were each flooded with approximately 2 $\times 10^{13}$ holes/cm^2. The enthalpy was determined from the slope of a plot of the natural logarithm of E' density versus reciprocal temperature, shown in Fig. 19; the activation enthalpy is approximately 1.5 ± 0.1 eV. To test the predictive capability of Eq. (15), holes were injected into samples subjected to each of the four annealing steps; mid-gap capacitance versus voltage shifts, ΔV_{mg}, were plotted versus injected hole fluence. Using expression (15) and taking the trapped holes to be close to the Si/SiO$_2$ boundary, our model[15] predicts mid-gap shifts of

$$\Delta V_{mg} = \frac{q\alpha e^{-\beta/T}}{C_{ox}} (1 - e^{\sigma\eta}), \qquad (16)$$

where q is electronic charge, C_{ox} is oxide capacitance, and all other parameters are as previously defined.

Figure 20 compares the experimental results and the predictions of Eq. (16). The correspondence between prediction and experiment is quite close. It clearly demonstrates something new and almost certainly useful: It is possible to pre-
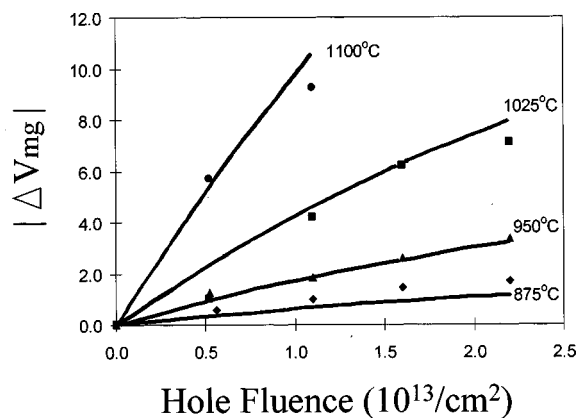
dict the response of an oxide from an essentially no-adjustable-parameter fit of a physically based model.

B. Predicting interface trap formation

Straightforward concepts from the equilibrium thermodynamics of chemical reactions also allow one to make some predictions about interface trap formation.[16]

As discussed previously at least four independent groups have demonstrated that significant (greater than or approximately equal to 10^{12}/cm^2) generation of P_b centers occurs when MOS oxides are subjected to technologically relevant levels of ionizing radiation. More limited results indicate P_b generation resulting from high or low oxide electric field injection of electrons as well as the injection of hot holes into the oxide from the near drain region of short channel MOS-FETS. The previously discussed studies of Conley et al.[57,58] show that E' centers react with molecular hydrogen at room temperature and that this reaction is accompanied by the simultaneous generation of Si/SiO$_2$ interface traps (these are P_b centers).

In our study,[57,58] only about 25% of the E' centers disappeared as about an equal number of hydrogen complexed E' centers (which we term E'H) appeared: the loss in E' density was accompanied by an approximately equivalent gain in interface trap density. No increase in interface trap density occurred with H$_2$ exposure if the positively charged E' centers were absent. These observations are significant because when SiO$_2$ is subjected to ionizing radiation, atomic hydrogen is created: above 110 °K it very rapidly dimerizes leaving behind H$_2$ in the oxide.[76]

It is well established that silicon dangling bond sites at the Si/SiO$_2$ interface (P_b centers) are passivated by hydrogen.[3,77] Assuming that the interface trap creation process involves the breaking of silicon–hydrogen bonds at P_b center precursor sites (P_bH) we proposed a reaction of the following form:[16]

$$H_2 + P_bH + E' \rightleftharpoons H_2 + P_b + E'H. \qquad (17)$$
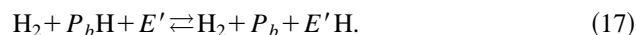
In this reaction, H$_2$ plays the formal role of a catalyst. When a hole drifting to an E' precursor site is captured, a positively charged silicon dangling bond site (E' center) is

created, which, as Conley *et al.*[58] have shown, can react with radiolytic H₂ to form a complex which we term E'H. After irradiation, the H₂ is eventually dissipated, but for a short time the system will *approach* equilibrium. Elementary statistical mechanics tells us that, if the system were to reach equilibrium, one could write[78]

$$\frac{[P_b][E'\text{H}]}{[P_b\text{H}][E']} = K, \tag{18}$$

where $K = \exp(-\Delta G/kT)$ and ΔG is the difference in Gibbs free energy of the reactants and products. Since expression (18) involves the transfer of a hydrogen atom from a silicon at the interface (P_b) to a silicon in the oxide (E'), one would reasonably conclude that ΔG is small. Thus, $K \cong 1$, at least within about an order of magnitude.

In order to solve Eq. (18) for ΔP_b (the concentration of P_b centers eventually generated after the interface trap formation process is complete) define the initial (prestress) P_b concentration to be P_{bi}, the initial (prestress) P_bH concentration to be $(P_b\text{H})_i$, and the density of E' trapped holes present immediately after irradiation (and immediately after all the holes which were not trapped are swept from the oxide) to be E'_1.

With these definitions, Eq. (19) becomes

$$\frac{[P_{bi} + \Delta P_b][\Delta P_b]}{[(P_b\text{H})_i) - \Delta P_b][E'_i - \Delta P_b]} = K. \tag{19}$$

In Eq. (19), take the number of E'H complex sites created to be equal to the number of P_b sites created. Assuming it captures the essential physics of the process, Eq. (19) predicts the interface trap generation behavior in a wide range of oxides.

For the technologically important situation in which the Si/SiO₂ interface has a very low interface trap and P_b density, $P_{bi} \cong 0$, at low dose $[\Delta P_b \ll (P_b\text{H})_i$, Eq. (19) becomes

$$\frac{[\Delta P_b][\Delta P_b]}{(P_b\text{H})_i(E'_i - \Delta P_b)} \cong K, \tag{20}$$

yielding

$$\Delta P_b \cong \frac{K}{2}(P_b\text{H})_i(\{1 + 4E'_i/[K(P_b\text{H})_i]\}^{1/2} - 1). \tag{21}$$

For a low level of initial E'_i generation ΔP_b will be almost equal (always slightly less than) the initial E'_i density. Thus, if we were to flood a very good oxide with a small number of holes, suppress the interface trap generation process, measure the initial trapped hole concentration, and then allow interface trap generation to proceed, we would expect that the eventual interface trap density (each P_b has two levels) would be roughly equal to the initial trapped hole density.

The generation of interface traps *can* be suppressed for hours by lowering the temperature of the system;[79] warming to room temperature allows the process to proceed. Many years ago, Hu and Johnson[79] subjected good oxide/silicon devices to relatively low levels of hole flooding at temperatures low enough to temporarily suppress interface trap gen-

eration. Initial oxide hole densities were evaluated, then interface traps allowed to generate, and those interface trap densities were also evaluated. As Eq. (21) predicts, Hu and Johnson found that the initial oxide hole density was approximately equal to the eventual interface trap density.

There are other semiquantitative aspects of this model which are in agreement with results in the literature.

(1) Expression (21) shows that ΔP_b should be sublinear in E'_i. Since E'_i generation should itself be sublinear in dose,[15] the model predicts a sublinear buildup of interface sites with dose. Such behavior is widely reported.[80]

(2) The model predicts that in devices with low initial interface trap density, the hole trapping and interface trap generation, P_b generation and E' generation would approximately scale together. This behavior (both cases) has been observed.[36]

(3) Since the model involves interaction of a trapped hole site with molecular hydrogen triggering a reaction at a Si/SiO₂ interface P_bH site, one would expect that the time involved in interface trap generation would be significantly increased by reversing the irradiation bias from positive gate voltage to negative gate voltage. This behavior is consistently observed.[81–83]

(4) Since the E' center precursors (oxygen vacancies) are intrinsic defects, one would expect that their number would be an exponential function of processing temperature. Thus one would expect a strong increase in interface trap generation with increasing temperature of gate oxide processing. This behavior is observed.[36]

(5) Radiolytic, molecular hydrogen will be rapidly dissipated from the oxide; in some cases this will not allow equilibrium densities of P_b interface traps to be achieved. One would thus expect that post irradiated exposure to a molecular hydrogen ambient generally increases interface trap density. This behavior is observed.[59,60]

(6) Consider a metal–oxide–semiconductor device in which the oxide has been flooded with holes for a brief period. If a positive voltage was applied to the gate electrode, E' precursors near the Si/SiO₂ boundary would be populated with holes: if a negative voltage was applied, E' precursors near the gate (usually polycrystalline Si/SiO₂ boundary) would be similarly populated. Our model, at least to zero order, predicts a similar radiation response, in that the eventual number of P_b centers created would be the same with either sign of gate bias during irradiation. (This assumes equal E' precursor density at both interfaces.) Experimental work indeed shows this to be the case ''electrically'' for brief bursts of irradiation *provided* that the oxide bias is positive *after* the irradiation.[83] (That is, the eventual interface state densities generated are approximately equal for both cases.)

(7) Briefly consider the technologically irrelevant case of a very high initial interface trap density and a very high initial P_b density. In such a case we would expect a reaction of the following form:

$$\text{H}_2 + P_b + E' \rightleftarrows E'\text{H} + P_b\text{H}. \tag{22}$$
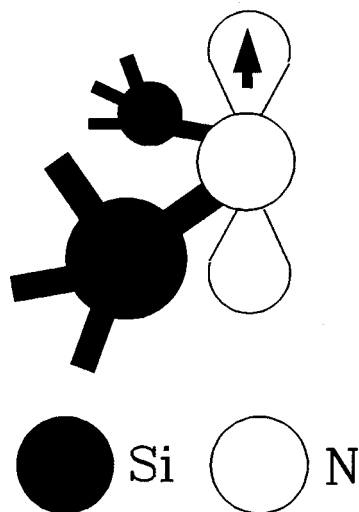
FIG. 21. Schematic illustration of the structure of the bridging nitrogen center.

Thus, the model would clearly predict an initial post irradiation *decrease* in P_b density for Si/SiO$_2$ structures with quite high initial P_b density. This behavior has been reported.[12]

XII. EXTRINSIC TRAPPING CENTERS

Often, impurity atoms (other than hydrogen) will be present in an oxide; nitrogen, phosphorous, and boron impurities have all been investigated to some extent in oxide films on silicon. Among these impurities, nitrogen appears to be of greatest potential significance.

A. Defect centers involving nitrogen

Chaiyesena *et al.*[84] and Yount *et al.*[85–88] have studied nitrogen defect centers in nitride and reoxidized, nitrided oxide films. Most of their work dealt with the bridging nitrogen center, N_b, illustrated in Fig. 21. An EPR trace due to this defect is illustrated in Fig. 22. A three line spectrum with each line of equal intensity is indicative of a spin-1 nucleus of approximately 100% abundance. Nitrogen is the only possibility. The center line is quite narrow, the two side peaks rather broad. This is so because quantum mechanics restricts the nitrogen nucleus to three orientations: parallel to the applied field, antiparallel to the applied field, and (any direction) perpendicular to the applied field. Since the perpendicu-
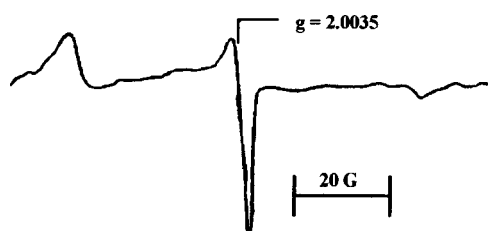

FIG. 22. EPR trace of the bridging nitrogen center.

lar orientation is not further specified, the center line effectively corresponds to no nuclear moment.

A straightforward analysis of the spectrum of Fig. 22 indicates an unpaired electron highly localized on a single nitrogen in a nearly pure p-type wave function. (Recall that the small splitting of the side peaks indicates quite low s character; their substantial breadth high p character.) The results clearly demonstrate that this center involves a nitrogen bonded to two other atoms, almost certainly silicons. The structure of the bridging nitrogen center is shown in Fig. 21. The bridging nitrogen EPR spectrum was first studied in large volume (~ 1 cm^3) samples by Mackey *et al.*[89] who also established the center's structural nature.

It should probably be mentioned that a very different EPR spectrum has been linked to bridging nitrogens by Stathis and Kastner.[90] Later studies by Tsai *et al.*[91] pointed out that the spectrum described by Stathis and Kastner[90] was incompatible with the bridging nitrogen hybridization and localization. Recently Austin and Leisure[92] have argued that the spectrum discussed by Stathis and Kastner[90] does not involve nitrogen at all but is caused by a carbon atom bonded to two hydrogens.

Chaiyasena *et al.*[84] and Yount *et al.*[85–88] identified the bridging nitrogen center as a rather large capture-cross-section electron trap. They found quite high densities of these centers in NH$_3$ annealed oxides ($\sim 10^{13}$/cm^3) and that their numbers are substantially reduced but not eliminated by reoxidation. Quite high densities of electron traps ($\sim 10^{13}$/cm^3) are found in NH$_3$ annealed oxides; their numbers are reduced but not eliminated by reoxidation. In N$_2$O annealed or N$_2$O grown oxides one finds far lower levels of both N$_B$ and electron traps. Yount *et al.*[85] provided quite direct evidence regarding the trapping capabilities of N$_B$ by showing that N$_B$ density is reduced when electrons are injected into the oxides. The N$_B$ capture cross section is about 10^{-15} cm^2. Yount *et al.*[85] noted that N$_B$ reacts rapidly with H$_2$ at room temperature. The N$_B$ signal is annihilated if the oxides under study are briefly exposed to H$_2$ at room temperature.

On the basis of these observations, Yount *et al.*[85–88] proposed that the precursor for N$_B$ is a nitrogen bonded to a hydrogen and two other atoms, presumably silicons and that the defect serves as an effective electron trap.

B. Defect centers involving phosphorous and boron

At least four phosphorous-related defect centers and one boron-related center have been identified in doped oxide films on silicon.[93–95] These centers have been studied in phosphosilicate glass (PSG) and borophosphosilicate glass (BPSG) films on silicon. The wide scan EPR trace of Fig. 23 illustrates the simultaneous presence of P_1, P_2, and P_4 centers along with the ubiquitous E' center and some organic free radicals in a tetraethyl orthosilicate (TEOS) based PSG thin film on silicon. A much narrower EPR trace taken on a silane based BPSG film indicated the simultaneous presence of the phosphorous oxygen hole center (POHC) in addition to the previously discussed P_{b0} and E' centers.
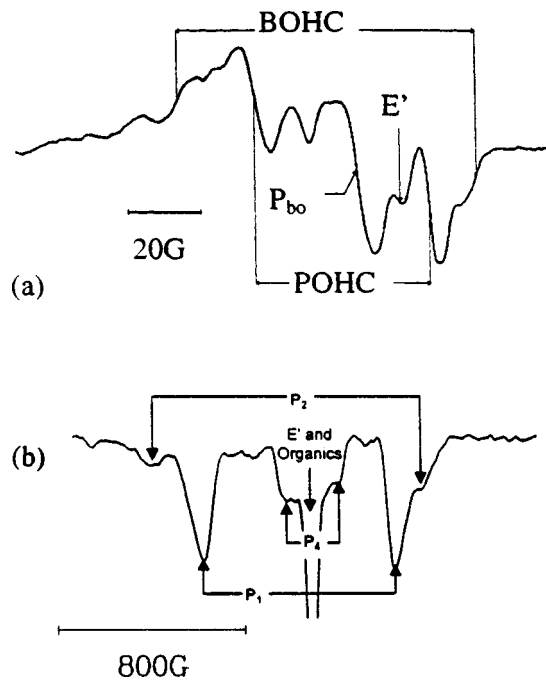
FIG. 23. EPR traces taken in (a) borophosphosilicate (BPSG) and (b) phosphosilicate (PSG) films showing (a) the boron oxygen hole center (BOHC) and phosphorous oxygen hole center (POHC) spectra superimposed upon the ubiquitous E' and P_b spectra and (b) the P_1, P_2, and P_4 spectra along with E' and organic radical spectra.

EPR parameters of the five centers are shown in Table I. Provisional defect structures (following Griscom *et al.*[96,97]) are illustrated in Fig. 24.

The literature on these phosphorous and boron centers in thin films is fairly limited.[93–95] They appear to play a role in instabilities in certain integrated circuits even though the BPSG and PSG films are typically interlevel dielectrics. Along with several organic centers, the phosphorous centers can capture significant amounts of space charge in the TEOS films.[95] Some of the phosphorous centers are also important charge trapping centers in silane based films.[93,94]

Limited studies of the response of P_1, P_2, and P_4 to the injection of charge carriers[94,95] into the oxide indicate that significant changes in the density of paramagnetic P_1, P_2, and P_4, and POHC centers occur when charge carriers are injected into the oxides in question; P_1, P_2, and POHC have large capture cross sections for holes, P_4 a large capture cross section for electrons.

C. Other paramagnetic centers in Si/SiO₂ systems

Several other paramagnetic centers have been observed in thin oxide films on silicon: unpaired electrons on oxygens,[98] (probably) nonbridging oxygens or peroxy centers, organic radicals,[95] and atomic hydrogen,[76] and electrically neutral E' centers.[65] Although radiolytic atomic hydrogen is clearly important since it is almost instantly dimerized to form molecular hydrogen at room temperature, studies of its presence in SiO₂ films on silicon are very limited. Studies of organic free radicals and the paramagnetic oxygen radical, have also been too limited to warrant further discussion.

TABLE I. EPR centers in oxide films: intrinsic and extrinsic defects.

Defect Name	EPR Parameters	Structure	Electronic Properties
(111) P_b	$g_\parallel = 2.0014$ $g_\perp = 2.008$ $A_{iso} = 110$ G $A_{aniso} = 21$ G	(Si structure)	Two broad levels in gap $U \cong 0.6$ eV
(100) P_{bo}	$g_1 = 2.0015 \cong g_\parallel$ $g_2 = 2.0080 \cong$ $g_3 = 2.0087 \cong g_\perp$ $A_{iso} = 96$ G $A_{aniso} = 24$ G	(Si structure)	Two broad levels in gap $U \cong 0.6$ eV
(100) P_{b1}	$g_1 = 2.0012$ $g_2 = 2.0076$ $g_3 = 2.0052$	(Si structure)	Two broad levels in gap $U \cong 0.3$ eV
E' (Positively Charged)	$g_\parallel = 2.0018$ $g_\perp = 2.0002$ $A_{iso} = 439$ G $A_{aniso} = 22$ G	(Si–O structure)	Deep hole trap Large hole capture cross section $\sigma \cong 3 \times 10^{-14}$ cm²
EP/E'_δ	g (zero cross) $\cong$ 2.0002 $A_{iso} = 120$ G $A_{aniso} =$ "small"	Provisional unrelaxed E' center	Deep hole trap Large hole capture cross section ($\sigma > \sigma (E')$)
E' (74 G doublet)	g (zero cross) $\cong$ 2.0016 A (H) $\cong$ 72 G	(Provisional) (Si–O–H structure)	At least sometimes positively charged. Created by H₂ interaction with E'
E' (10.4 G doublet)	$g_\parallel = 2.0018$ $g_\perp = 2.0002$ A (H) $\cong$ 13 G	(Provisional) (Si–O structure)	Created by H₂ interactions with E'
N_b	$g_\parallel = 2.0035$ $g_\perp = 2.0068$ $A_{iso} = 11$ G $A_{aniso} = 12.5$ G	(Si–N structure)	Neutral electron trap $\sigma \cong 10^{-15}$ cm²
P_1	$g_\parallel \cong g_\perp \cong 2.005$ $A_{iso} = 910$ G $A_{aniso} = 60$ G	(O–P structure)	When paramagnetic, it is a hole trap
P_2	$g \cong 2.0013$ $A_{iso} = 1110$ G $A_{aniso} = 50$ G	(O–P structure)	When paramagnetic, it is a hole trap
P_4	$g \cong 2.00$ $A_{iso} \cong 103$ G $A_{aniso} \cong 103$ G	(O–P structure)	Electron trap
POHC	$g_1 \cong 2.0075$ $g_2 \cong 2.0097$ $g_3 \cong 2.0179$ $A_1 = 48$ G $A_2 = 54$ G $A_3 = 51$ G	(O–P–O structure)	Hole trap
BOHC	$g_1 \cong 2.0025$ $g_2 \cong 2.0115$ $g_3 \cong 2.0355$ $A_1 = 13.6$ G $A_2 = 15.3$ G $A_3 = 8.7$ G	(Si–O–B–O structure)	Does not have a large capture cross section for electrons or holes

XIII. CONCLUSIONS

More than a dozen paramagnetic centers have been observed in MOS systems. Several of these centers play dominant roles in MOS device instabilities. Recent studies show that predictions with regard to oxide reliability can be made by combining our EPR-derived understanding of electrically active defects with fundamental principles of statistical mechanics. The various oxide centers and their properties are summarized in Table I.
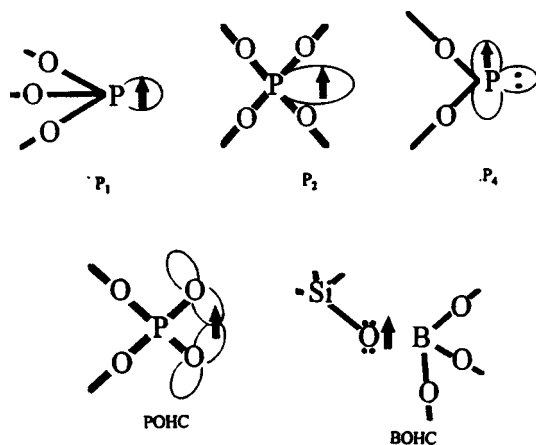
FIG. 24. Schematic sketch of phosphorous and boron centers found in PSG and BPSG thin films on silicon.

[1] J. H. Weil, J. R. Bolton, and J. E. Wertz, *Electron Paramagnetic Resonance: Elementary Theory and Practical Applications* (Wiley, New York, 1994).

[2] Y. Nishi, Jpn. J. Appl. Phys. **10**, 52 (1971).

[3] Y. Nishi, T. Tanaka, and A. Ohwada, Jpn. J. Appl. Phys. **11**, 85 (1972).

[4] P. J. Caplan, E. H. Poindexter, B. E. Deal, and R. R. Razouk, J. Appl. Phys. **50**, 879 (1979).

[5] E. H. Poindexter, P. J. Caplan, B. E. Deal, and R. R. Razouk, J. Appl. Phys. **52**, 879 (1981).

[6] P. M. Lenahan, K. L. Brower, P. V. Dressendorfer, and W. C. Johnson, IEEE Trans. Nucl. Sci. **28**, 4105 (1981).

[7] P. M. Lenahan and P. V. Dressendorfer, Appl. Phys. Lett. **41**, 542 (1982).

[8] P. M. Lenahan and P. V. Dressendorfer, J. Appl. Phys. **55**, 3495 (1984).

[9] Y. Y. Kim and P. M. Lenahan, J. Appl. Phys. **64**, 3551 (1988).

[10] R. L. Vranch, B. Henderson, and M. Pepper, Appl. Phys. Lett. **52**, 1161 (1988).

[11] H. Miki, M. Noguchi, K. Yokogawa, B. Kim, K. Asada, and T. Sugano, IEEE Trans. Electron Devices **35**, 2245 (1988).

[12] K. Awazu, W. Watanabe, and H. Kawazoe, J. Appl. Phys. **73**, 8519 (1993).

[13] T. Takahashi, B. B. Triplett, K. Yokogawa, and T. Sugano, Appl. Phys. Lett. **26**, 1339 (1987).

[14] W. Carlos, Nucl. Instrum. Methods Phys. Res. B **1**, 383 (1984).

[15] P. M. Lenahan, J. F. Conley, Jr., and B. D. Wallace, J. Appl. Phys. **81**, 6824 (1997).

[16] P. M. Lenahan and J. F. Conley, Jr., Appl. Phys. Lett. **71**, 3128 (1997).

[17] J. F. Conley, Jr. and P. M. Lenahan in *The Physics and Chemistry of SiO₂ and the Si/SiO₂ Interface III*, Proceedings of the Electrochemical Society, edited by H. Z. Massoud, E. H. Poindexter, and C. R. Helms (Electrochemical Society, Pennington, NJ, 1996), Vol. 96-1, p. 214.

[18] J. H. Stathis and L. Dori, Appl. Phys. Lett. **58**, 1641 (1991).

[19] E. Cartier and J. H. Stathis, Microelectron. Eng. **28**, 3 (1995).

[20] C. P. Slichter, *Principles of Magnetic Resonance*, 2nd ed. (Springer, Berlin 1978), Chap. 4.

[21] H. A. Schafft, D. A. Baglee, and P. E. Kennedy, Proceedings of the IEEE International Reliability Symposium (IRPS), 1991, pp. 1–7.

[22] K. L. Brower, Appl. Phys. Lett. **43**, 1111 (1983).

[23] M. A. Jupina and P. M. Lenahan, IEEE Trans. Nucl. Sci. **37**, 1650 (1990).

[24] J. W. Gabrys, P. M. Lenahan, and W. Weber, Microelectron. Eng. **22**, 273 (1993).

[25] J. L. Cantin, M. Schoisswohl, H. J. von Bardeleben, V. Morazzani, J. J. Ganem, and I. Trimaille, in *The Physics and Chemistry of SiO₂ and the Si/SiO₂ Interface III*, Proceedings of the Electrochemical Society, edited by H. Z. Massoud, E. H. Poindexter, and C. R. Helms (The Electrochemical Society, Pennington, NJ, 1996), Vol. 96-1, p. 28.

[26] K. L. Brower, Z. Phys. Chem., Neue Folge **151**, 177 (1987).

[27] E. H. Poindexter, P. J. Caplan, J. J. Finegan, N. M. Johnson, D. K. Biegelson, and M. D. Moyer, in *The Physics and Technology of MOS Insulators*, edited by G. Lucovsky, S. T. Panelides, and F. L. Galeener (Pergamon, New York, 1980), p. 326.

[28] C. Brunstrom and C. V. Svensson, Solid State Commun. **37**, 339 (1981).

[29] E. H. Poindexter, G. J. Gerardi, M. E. Ruekel, P. J. Caplan, N. M. Johnson, and D. K. Biegelson, J. Appl. Phys. **56**, 2844 (1984).

[30] G. J. Gerardi, E. H. Poindexter, P. J. Kaplan, and N. M. Johnson, Appl. Phys. Lett. **49**, 348 (1986).

[31] D. J. Lepine, Phys. Rev. B **6**, 436 (1972).

[32] A. S. Grove and D. J. Fitzgerald, Solid-State Electron. **9**, 783 (1966).

[33] D. J. Fitzgerald and A. S. Grove, Surf. Sci. **9**, 347 (1968).

[34] E. H. Snow, A. S. Grove, and D. J. Fitzgerald, Proc. IEEE **55**, 1168 (1967).

[35] J. Dong and D. Drabold, Phys. Rev. Lett. **80**, 1928 (1998).

[36] P. M. Lenahan and P. V. Dressendorfer, IEEE Trans. Nucl. Sci. **30**, 4602 (1983).

[37] R. E. Mikawa and P. M. Lenahan, J. Appl. Phys. **59**, 2054 (1986).

[38] W. L. Warren and P. M. Lenahan, Appl. Phys. Lett. **49**, 1296 (1986).

[39] J. T. Krick, P. M. Lenahan, and G. J. Dunn, Appl. Phys. Lett. **59**, 3437 (1991).

[40] T. E. Tsai, D. L. Griscom, and E. J. Friebele, Phys. Rev. B **40**, 6374 (1989).

[41] P. S. Winokur and H. E. Boesch, Jr., IEEE Trans. Nucl. Sci. **NS-28**, 4088 (1981).

[42] P. S. Winokur, J. M. McGarrity, and H. E. Boesch, Jr., IEEE Trans. Nucl. Sci. **NS-23**, 1580 (1976).

[43] N. M. Johnson, in *Hydrogen in Semiconductors*, edited by J. Pankove and N. M. Johnson (Academic, San Diego, 1991), p. 113.

[44] E. Cartier, J. H. Stathis, and D. A. Buchanan, Appl. Phys. Lett. **63**, 1510 (1993).

[45] C. R. Viswanathan and J. Maserjian, IEEE Trans. Nucl. Sci. **NS-23**, 1540 (1976).

[46] G. F. Derbenwick and B. L. Gregory, IEEE Trans. Nucl. Sci. **NS-22**, 2151 (1975).

[47] N. S. Saks, M. G. Ancona, and J. A. Modolo, IEEE Trans. Nucl. Sci. **NS-33**, 1185 (1986).

[48] R. H. Silsbee, J. Appl. Phys. **32**, 1459 (1961).

[49] F. J. Feigl, W. B. Fowler, and K. L. Yip, Solid State Commun. **14**, 225 (1974).

[50] P. M. Lenahan and P. V. Dressendorfer, IEEE Trans. Nucl. Sci. **29**, 1459 (1982).

[51] C. L. Marquardt and G. H. Sigel, Jr., IEEE Trans. Nucl. Sci. **22**, 2234 (1975).

[52] T. Takahashi, B. B. Triplett, K. Yokogawa, and T. Sugano, Appl. Phys. Lett. **26**, 1334 (1987).

[53] B. B. Triplett, T. Takahishi, and T. Sugano, Appl. Phys. Lett. **50**, 1663 (1987).

[54] L. Lipkin, L. Rowan, A. Reisman, and C. K. Williams, J. Electrochem. Soc. **138**, 2050 (1991).

[55] T. E. Tsai and D. L. Griscom, J. Non-Cryst. Solids **91**, 170 (1987).

[56] J. Vitko, J. Appl. Phys. **49**, 5530 (1978).

[57] J. F. Conley, Jr. and P. M. Lenahan, IEEE Trans. Nucl. Sci. **39**, 2186 (1992).

[58] J. F. Conley, Jr. and P. M. Lenahan, IEEE Trans. Nucl. Sci. **40**, (1993).

[59] R. A. Kohler, R. A. Kushner, and K. H. Lee, IEEE Trans. Nucl. Sci. **35**, 1492 (1988).

[60] R. E. Stahlbush, B. J. Mrstik, and R. K. Lawrence, IEEE Trans. Nucl. Sci. **37**, 1641 (1990).

[61] J. F. Conley, Jr., P. M. Lenahan, and P. Roitman, IEEE Trans. Nucl. Sci. **39**, 2114 (1992).

[62] J. F. Conley, Jr., P. M. Lenahan, and P. Roitman, Appl. Phys. Lett. **60**, 2889 (1992).

[63] W. L. Warren, M. R. Shaneyfelt, J. R. Schwank, D. M. Fleetwood, P. S. Winokur, R. A. B. Devine, W. P. Maszara, and J. B. McKitterick, IEEE Trans. Nucl. Sci. **40**, 1755 (1993).

[64] K. Vanheusden and A. Stesmans, J. Appl. Phys. **74**, 275 (1993).

[65] J. F. Conley, Jr., P. M. Lenahan, H. L. Evans, R. K. Lowry, and T. J. Morthorst, J. Appl. Phys. **76**, 2872 (1994).

[66] J. F. Conley, Jr. and P. M. Lenahan, Microelectron. Eng. **28**, 35 (1995).

[67] L. Zhang and G. G. Leisure, J. Appl. Phys. **80**, 3744 (1996).

[68] J. R. Chavez, S. P. Karna, K. Vanheusden, C. P. Brothers, R. D. Pugh, B. K. Singaraju, W. L. Warren, and R. A. B. Devine, IEEE Trans. Nucl. Sci. **NS-44**, 1799 (1997).

[69]A. J. Lelis, H. E. Boesch, Jr., T. R. Oldham, and F. B. McLean, IEEE Trans. Nucl. Sci. **35**, 1186 (1988).

[70]A. J. Lelis, Jr., T. R. Oldham, H. E. Boesch, and F. B. McLean, IEEE Trans. Nucl. Sci. **36**, 1186 (1989).

[71]J. F. Conley, Jr., P. M. Lenahan, A. J. Lelis, and T. R. Oldham, Appl. Phys. Lett. **67**, 2179 (1995).

[72]W. L. Warren, M. R. Shaneyfelt, D. M. Fleetwood, J. R. Schwank, and P. S. Winokur, IEEE Trans. Nucl. Sci. **41**, 1817 (1994).

[73]B. Henderson, *Defects in Crystalline Solids* (Crane-Russek, New York, 1972), Chap. 1.

[74]Y. M. Chaing, D. P. Birnie III, and D. M. Kingery, *Physical Ceramics*, (Wiley, New York, 1997), Chap. 2.

[75]T. Ohmameuda, H. Miki, K. Asada, T. Sugano, and Y. Ohji, Jpn. J. Appl. Phys., Part 2 **30**, L1993 (1991).

[76]K. L. Brower, P. M. Lenahan, and P. V. Dressendorfer, J. Appl. Phys. **41**, 251 (1982).

[77]K. L. Brower, Phys. Rev. B **38**, 9657 (1988).

[78]L. Pauling, *General Chemistry* (Dover, New York, 1988).

[79]G. J. Hu and W. C. Johnson, J. Appl. Phys. **54**, 1441 (1983).

[80]T. P. Ma and P. V. Dressendorfer, *Ionizing Radiation Effects in MOS Devices and Circuits* (Wiley, New York, 1989), and references therein.

[81]F. B. McLean, IEEE Trans. Nucl. Sci. **NS-27**, 1651 (1981).

[82]N. S. Saks and M. G. Ancona, IEEE Trans. Nucl. Sci. **NS-34**, 1348 (1987).

[83]H. E. Boesch, IEEE Trans. Nucl. Sci. **NS-35**, 1160 (1988).

[84]J. A. Chaiyasena, P. M. Lenahan, and G. J. Dunn, Appl. Phys. Lett. **58**, 2141 (1991).

[85]J. T. Yount, P. M. Lenahan, and G. J. Dunn, IEEE Trans. Nucl. Sci. **39**, 2211 (1992).

[86]J. T. Yount and P. M. Lenahan, J. Non-Cryst. Solids **164−66**, 1069 (1993).

[87]J. T. Yount, P. M. Lenahan, and J. T. Krick, J. Appl. Phys. **76**, 1754 (1994).

[88]J. T. Yount, Ph.D. thesis, The Pennsylvania State University, 1995.

[89]J. H. Mackey, J. W. Boss, and M. Kopp, Phys. Chem. Glasses **II**, 205 (1970).

[90]J. H. Stathis and M. A. Kastner, Phys. Rev. B **29**, 7079 (1984).

[91]T. E. Tsai, D. L. Griscom, and E. J. Friebele, Phys. Rev. B **38**, 2140 (1988).

[92]W. R. Austin and R. G. Leisure, Phys. Rev. B **54**, 15064 (1996).

[93]W. L. Warren, M. R. Shaneyfelt, D. M. Fleetwood, P. S. Winokur, and S. Montague, IEEE Trans. Nucl. Sci. **NS-42**, 1731 (1995).

[94]R. Fuller, H. Evans, C. Gamlin, B. Czagas, M. Morrison, D. Decrosta, R. Lowry, P. M. Lenahan, and C. J. Frye, IEEE Trans. Nucl. Sci. **43**, 2565 (1996).

[95]C. A. Billman, P. M. Lenahan, R. Fuller, H. Evans, W. H. Speece, D. DeCrosta, and R. Lowry, IEEE Trans. Nucl. Sci. **44**, 1834 (1997).

[96]D. L. Griscom, E. J. Friebele, K. J. Long, and J. W. Fleming, J. Appl. Phys. **43**, 960 (1976).

[97]D. L. Griscom, G. H. Sigel, Jr., and R. J. Ginther, J. Appl. Phys. **54**, 3743 (1983).

[98]P. M. Lenahan and P. V. Dressendorfer, IEEE Trans. Nucl. Sci. **NS-29**, 1459 (1982).